Supplementary information

Genomic inference of a human super bottleneck in the Early Stone Age

Wangjie Hu[1,†], Ziqian Hao[1,†], Pengyuan Du[1], Yi-Hsuan Pan[2,*], Haipeng Li[1,3,*]

[1]CAS Key Laboratory of Computational Biology, Shanghai Institute of Nutrition and Health, University of Chinese Academy of Sciences, Chinese Academy of Sciences, Shanghai 200031, China.

[2]Key Laboratory of Brain Functional Genomics of Ministry of Education, School of Life Science, East China Normal University, Shanghai 200062, China.

[3]Center for Excellence in Animal Evolution and Genetics, Chinese Academy of Sciences, Kunming 650223, China.

†These authors contributed equally.

*Corresponding Authors: yxpan@sat.ecnu.edu.cn; lihaipeng@picb.ac.cn

Table of Contents

List of figures

List of tables

List of Symbols

Symbol	Meaning
$N(\cdot)$	Demographic history, or varying population size.
t	Standard coalescent time (scaled by $2N(t)$ generations).
τ	One-point scaled time (scaled by $2N(0)$ generations).
n	Sample size, or the number of sampled chromosomes.
l	State (the number of lineages).
$p_l(t)$	Probability of state l at time t.
i	Size of branch.
$BL_i(N(\cdot))$	Expected branch length of size i given population size, in number of generations.
$\vec{\xi} = (\xi_i)$	SFS, $i = 1, \cdots, n-1$. ξ_i is the number of mutations with size i. ξ_1 is usually called the number of singletons, and ξ_2 the number of doubletons.
$\{t_0, t_1, \cdots, t_m\}$	Time partition, and $0 = t_0 < t_1 < \cdots < t_m$.

Validation of FitCoal calculation

We verified the calculation of expected branch lengths in this section. Under the constant size model, when the sample size was small ($n = 5$, where n is the number of sequences) or extremely large ($n = 1{,}000$), FitCoal calculated the expected branch lengths correctly[1] (Table S13). Computational accuracy reached 10^{-8} or 10^{-11}. The high accuracy is important for the precise estimation of demographic history in the following sections.

Moreover, our results were almost the same as the expected branch lengths under three simple models calculated by using the Zivković-Wiehe method[2] (Table S14). Since Zivković-Wiehe equations can be numerically solved when $n < 50$, we could not compare our results with theirs when the sample size was large.

For more complex models, the average branch lengths were obtained from extensive coalescent simulations. Although with certain variances, the simulated results were

consistent with the FitCoal expected branch lengths under different demographic models (Table S15). Therefore, FitCoal can analytically derive the expected branch length for each SFS type under arbitrary demographic models.

We also compared the results obtained from the tabulated FitCoal and those from the original ones without tabulation. These results were nearly identical with each other (Tables S14 and S15). Since the former was much faster than the latter, the former was used to infer demographic histories. Hereafter, tabulated FitCoal is referred to as FitCoal for short, unless otherwise indicated.

SFS truncation

Denote the SFS of n samples by $\vec{\lambda} = (\lambda_1, \dots, \lambda_{n-1})$. An m-dimension vector $\vec{V} = (v_1, \dots, v_m)$ is said to be tail-up if there exist $z \in \{1, \cdots, m-1\}$ such that $v_z < \cdots < v_m$. If $\vec{\lambda}$ is the expected SFS of a single varying size population, we have $\lambda_{\lceil n/2 \rceil} > \cdots > \lambda_{n-1}$. However, the observed SFS $\vec{\xi} = (\xi_1, \dots, \xi_{n-1})$ may be tailed up because of some evolutionary factors, such as positive selection and population structure, which could introduce bias to the demographic inference. Therefore, the truncated SFS is recommended.

A simple procedure is implemented to discard the tail-up types of SFS, containing high-frequency mutations. To determine the truncated tail of SFS, a small window slides through the SFS. The cutoff is determined if ξ_i exceeds its random fluctuation range. Let

$$\hat{n}(\vec{\xi}) = \max_{k \in \{1,\cdots,n-1\}} \left\{ k \middle| \overline{w}_k(\vec{\xi}) - 3SD_k(\vec{\xi}) < w_{k-i(n)+1}, \cdots, w_k < \overline{w}_k(\vec{\xi}) + 3SD_k(\vec{\xi}) \right\},$$

where $\overline{w}_k(\vec{\xi}) = \frac{1}{i(n)} \sum_{a=k-i(n)+1}^{k} \xi_a$, $SD_k(\vec{\xi}) = \sqrt{\overline{w}_k(\vec{\xi})}$, and $i(n) = \begin{cases} 3 & n \le 50 \\ 4 & 50 < n \le 100 \\ 5 & n > 100 \end{cases}$.

The truncated SFS $\vec{\xi}^T = (\xi_i)$, where $i = 1, \cdots, k$. In the analysis, we used this strategy to truncate the SFS for each human population. We call $(n-k)/n$ the proportion of truncated SFS types.

When the truncating strategy was applied, the proportion of truncated SFS types was different for different populations (Table S5, S7). Therefore, to verify the effect of this strategy, the same truncating standard (~10%, the mean proportion) was also used for

1000GP populations (Fig. S10). For HGDP-CEPH, because the proportion of considered SNPs without missing samples is larger than 80% for all populations, we used the corresponding SFS to determine the cutoff to truncate both SFSs. Similarly, the same truncating standard (~15%, the mean proportion) was used for HGDP-CEPH (Fig. S10).

Composite likelihood

Denote μ as the mutation rate per base pair per generation. Denote $\vec{\xi} = (\xi_i)$ as the observed number of SNPs of n sequences with σ base pair, where $i = 1, \cdots, n-1$. The expected SFS $\vec{\lambda} = (\lambda_i)$, where $\lambda_i = \mu\sigma BL_i(N(\cdot))$, . Following the Poisson probability and the previous studies[3,4], the composite likelihood could be written as

$$L_{\mu,\iota}(\vec{\xi}, N(\cdot)) = \prod_{i=1}^{n-1} \frac{\lambda_i^{\xi_i} e^{-\lambda_i}}{\xi_i!}.$$

For missing data, we assume that $\sigma^{(n)}$ base pair are sequenced in n samples and S is the set of all sample sizes. We denote the observed number of SNPs of $n(\in S)$ sequences by $\vec{\xi}^{(n)} = \left(\xi_1^{(n)}, \cdots, \xi_{n-1}^{(n)}\right)$. The expected SFS of n sequences $\vec{\lambda}^{(n)} = \left(\lambda_1^{(n)}, \cdots, \lambda_{n-1}^{(n)}\right)$, where $\lambda_i^{(n)} = \mu\sigma^{(n)} BL_i^{(n)}(N(\cdot))$, $BL_i^{(n)}(N(\cdot))$ is the expected branch length of type i with n samples under population size $N(\cdot)$. Total number of base pair is given by $\sigma(S) := \sum_{n\in S} \sigma^{(n)}$. The composite likelihood could be written as

$$\begin{aligned} & L_{\mu,(\iota^{(n)})_{n\in S}}((\vec{\xi}^{(n)})_{n\in S}, N(\cdot)) \\ &= \prod_{n\in S} L_{\mu,\iota^{(n)}}(\vec{\xi}^{(n)}, N(\cdot)) \\ &= \prod_{n\in S} \prod_{i=1}^{n-1} \frac{(\lambda_i^{(n)})^{\xi_i^{(n)}} e^{-\lambda_i^{(n)}}}{\xi_i^{(n)}!} \end{aligned}.$$

If SFS is tail-up, we use truncated SFS $\vec{\xi}^{T} = (\xi_i)$, where $i = 1, \cdots, k$. The composite likelihood is

$$L_{\mu,\iota}(\vec{\xi}^{T}, N(\cdot)) = \prod_{i=1}^{k} \frac{\lambda_i^{\xi_i} e^{-\lambda_i}}{\xi_i!}.$$

Sequencing errors often affect rare mutations in a sample. Thus singletons and mutations with size $(n-1)$ can be discarded. Although this is unnecessary in this study, as a general method, the composite likelihood of an SFS without those mutations is

$$L_{\mu,\iota}(\vec{\xi}, N(\cdot)) = \prod_{i=2}^{n-2} \frac{\lambda_i^{\xi_i} e^{-\lambda_i}}{\xi_i!}.$$

FitCoal- and simulation-based likelihood surface

In this section, we compared two likelihood surfaces based FitCoal and simulation (Fig. S1). We considered an instantaneous growth model. The population size increases from 10,000 (N_1) to 20,000 (N_0) at standard coalescent time 0.2. For simplicity, we obtained a SFS by multiplying the expected branch length by θl ($= 4\mathrm{N}_0\mu$), where $\mu l = 1.0$. The number of sequences is 100.

We then compared the FitCoal composite likelihood surface of the SFS and the composite likelihood surface of the SFS based on simulation approach. To draw the likelihood surfaces, we performed a grid search in a parameter space. We considered that the population size increase from N_1 to N_0 at standard coalescent time 0.2, where N_0 ranges from 19,600 to 20,400 and N_1 from 9,800 to 10,200. The coalescent simulations were conducted by the ms software. The number of simulations is 100,000 to calculate the simulation-based likelihood.

The surface of FitCoal likelihood is smooth, but the surface of likelihood based on simulation approach is rugged (Fig. S1). Moreover, the FitCoal likelihoods are also larger than those based on simulation approach because the FitCoal expected branch lengths fit the data better than the average branch lengths obtained from simulations.

Demographic inference on simulated data

It has been shown that FitCoal can precisely estimate the demographic histories under six different demographic models (Fig. 2). We then validated the accuracy of FitCoal on more simulated data in this section.

Comparing with the examined cases (Fig. 2), the performance of FitCoal can be further improved by providing a priori knowledge. In some circumstances, a slow and continuous change may be more biological relevant than a quick and sudden change and vice versa. FitCoal was then re-performed conditional on either exponential or instantaneous change within each inference time interval (Fig. S14 and S15). Our results

showed that the FitCoal accuracy was enhanced in the presence of correct priori knowledge. Even if the condition was misspecified, the inferred demographic histories were still similar with the true histories.

FitCoal is a model-flexible method and the number of inference time intervals is dependent on the complexity of true demography. FitCoal has the power to detect more complex population histories (Fig. S16). Although FitCoal may omit slight changes of population size occurred in short time periods, it has great ability to detect the major changes in all examined complex histories. When two-population split models are considered (Fig. S17), FitCoal is reasonably accurate but with a slightly larger recent population size due to the effects of migration.

Effects of positive selection

To simulate samples affected by positive selection, we considered a two-locus model[5] under a constant size model. We assumed that the effective population size was 27,000, and the number of neutral fragments were 10,000, and 10 or 20% of them were partially linked with selected alleles. The distance between the neutral and the selected loci was 50kb, and recombination rate was 1cM per Mb. The sample size was 202 (the average sample size of 1000GP populations). The selection coefficient (s = 0.01 or 0.05) was varied. We assumed a mutation rate of 1.2×10^{-8} per base per generation and a generation time of 24 years. To compare among different cases, the fixed number SNPs (5,882,885 SNPs, the average number of SNPs in 1000GP populations) were applied. Under neutrality, it was equivalent to the sequenced length of 771.589 Mb.

All the simulated samples had a tail-up feature because of the excess of high-frequency mutations[6]. Considering the low genetic diversity of selected loci, the contribution of selected loci to the genome-wide diversity was relatively low, thus only a slight excess of rare mutations[7] was observed. The ratio between the number of singletons and doubletons ranged between 2.01 and 2.10 in the simulated samples, only slightly larger than the expected value (2.0) under neutrality.

We then applied FitCoal to estimated demography. When the full SFSs were used, our results showed that the population size remains constant within 2,000 kry (Fig. S5a). If the selection strength was greatly strong ($s = 0.05$, where s is the selection coefficient),

FitCoal estimated a large ancient population ~240 kyr ago because of the effects of high-frequency mutations. When the high-frequency mutations were removed (*i.e.* the truncated SFS), the large ancient population size was reduced (Fig. S5b). If $s = 0.01$ and 20% loci were subject to positive selection, a slight population expansion was observed, corresponding to the slight excess of rare mutations due to positive selection. Overall, a correct demographic history was estimated within two million years.

Verification of inferred human demographic histories

To evaluate the precision of the inferred human demographic histories (Fig. 3), we simulated 200 data sets under each demographic history. The results showed that FitCoal, with truncated SFS, is highly accurate to reveal human demographic history (Fig. S18 – S28). Moreover, when high-frequency mutations were discarded, the truncated proportion of SFS was different for different populations. To address the influence of truncated proportions, we inferred the demographic histories by setting the average truncating proportion within each data set (10% for 1000GP and 15% for HGDP-CEPH) (Fig S10). Results were consistent with the ones obtained above. Therefore, the strategy of truncating SFS does not affect our conclusions.

Similar with the log-likelihood ratio test, the number of inference time intervals was determined by the log-likelihood promotion rate when increasing the number of inference time intervals. It is recommended to use 20% as the threshold of log-likelihood promotion rate derived from extensive simulation results (Table S11). When analyzing the human data, the inferred demographic histories are not sensitive to this threshold (Fig. S29, S30; Tables S16, S17). For example, the log-likelihood promotion rate for three and four inference time intervals of CEU is 2471.16 and 17.07%, respectively. The number of inference time intervals is three, and the inferred demographic history is highly similar with that with four inference time intervals. Thus, the inferred demographic histories are robust to the threshold of 20%.

Alternative hypotheses of the super bottleneck

In this study, the super bottleneck is detected in all the 10 African populations, but not in all the 40 non-African populations. Two alternative hypotheses were explored. First, the super bottleneck was a false positive result due to positive selection. However, FitCoal did not falsely estimate a bottleneck due to the existence of positive selection (Fig. S5). Besides all the 40 non-African populations could also be affected by positive selection, but no super bottleneck was found. Thus it is unlikely that the bottleneck is a false positive bias introduced by positive selection. Second, the super bottleneck could occur in the African populations after the non-African populations were derived. This requires that the African and non-African populations diverged before 1,000 kyr ago, which makes the hypothesis impossible. Therefore, the super bottleneck is shared by African and non-African populations.

Loss of genetic diversity due to the super bottleneck

To measure the loss of current human genetic diversity due to the super bottleneck, we calculated the expected tree length of demographic histories with or without the super bottleneck. It was straightforward to ignore a bottleneck with instantaneous size changes, thus we considered seven 1000GP African populations (ACB, ASW, ESN, GWD, LWK, MSL and YRI) and one HGDP-CEPH African population (Yoruba). To remove the bottleneck, we replaced the population size during the super bottleneck with that after the bottleneck. We then compared the expected tree length of inferred demographic history (ω_1) with that of demographic history without the bottleneck (ω_0).

The loss of current genetic diversity due to the super bottleneck is $(\omega_0 - \omega_1)/\omega_0$. When the actual sample size was used for each population, the genetic diversity was measured as Watterson's θ. The genetic diversity loss of these eight populations was 46.22% and the range was 32.17–60.56%.

When $n = 2$, the genetic diversity was measured as π, the pairwise nucleotide diversity. The loss of current genetic diversity in these eight populations was 65.85% and the range was 52.71–73.60%. It was larger than the estimate based on Watterson's θ because the bottleneck was ancient and the recovery rate of Watterson's θ was faster than

that of π^8. These results demonstrate the importance of the super bottleneck in the human evolution.

The super bottleneck estimated in Africans

In this section, we explored why the super bottleneck can only be estimated in the African population and provided the mathematical explanation. We proved that the inferred number of intervals before time t depends on the dimension of the SFS before time t.

Denote the probability of state l at time t from n samples by $p_l^n(t)$, where $l = 2, \cdots, n$. And denote the expected brach length of size i from n samples by $BL_i^n(N(\cdot))$, where $i = 1, \cdots, n-1$. There exists an invertible matrix $\mathcal{X} = \left(x_g^h\right)_{g,h=2,\cdots,n}$ which only depends on n, such that $p_l^n(t) = \sum_{g=2}^{n} x_g^l \, p_g^g(t)$ (ref.[9,10]). If positive numbers $m < n$, there exist a matix $\mathcal{Y} = \left(y_g^h\right)_{g=2,\cdots,m,h=2,\cdots,n}$, which only depends on m and n, such that $p_l^m(t) = \sum_{h=2}^{n} y_l^h \, p_h^n(t)$. Combined with eq(1), there exist a matrix $\mathcal{Z} = \left(z_g^h\right)_{g=1,\cdots,m-1,h=1,\cdots,n-1}$, which only depends on m and n, such that $BL_i^m(N(\cdot)) = \sum_{j=1}^{n-1} z_i^j \, BL_j^n(N(\cdot))$.

Define the population size before time t by $N^t(s) = N(t+s)$. Denote the expected branch length of state l before time t by $B_l(t) = \left(b_{1,l}(t), \cdots, b_{l-1,l}(t)\right)$, where $b_{i,l}(t)$ represent the expected branch length of state l before time t of type i at time t. We have $b_{j,l}(t) = p_l^n(t) BL_j^l(N^t(\cdot))$. $BL_{i,k}^t$ ($i = 1, \cdots, n-1$) denote the branch length of type i whose number of lineages are no more than k before time t. We have

$$BL_{i,k}^t = \sum_{l=2}^{k} \sum_{j=1}^{l-1} \frac{p(j \to i) p(l-j \to n-i)}{p(l \to n)} b_{j,l}(t),$$

$$\text{where } p(a \to b) = \begin{cases} \binom{b-1}{a-1} & b \geq a \geq 1 \\ 0 & \text{else} \end{cases}.$$

Then,

$$
\begin{aligned}
& BL_{i,k}^{t} \\
= \; & \sum_{l=2}^{k}\sum_{j=1}^{l-1}\frac{p(j\to i)p(l-j\to n-i)}{p(l\to n)}b_{j,l}(t) \\
= \; & \sum_{l=2}^{k}\sum_{j=1}^{l-1}\frac{p(j\to i)p(l-j\to n-i)}{p(l\to n)}p_{l}^{n}(t)BL_{j}^{l}(N^{t}(\cdot)) \\
= \; & \sum_{h=1}^{k-1}\Big(\sum_{l=2}^{k}\sum_{j=1}^{l-1}\frac{p(j\to i)p(l-j\to n-i)}{p(l\to n)}p_{l}^{n}(t)z_{j}^{h}\Big)BL_{h}^{k}(N^{t}(\cdot))
\end{aligned}
\qquad (332)
$$

Thus, the space that is generated by $BL_{1,k}^{t}$, $\cdots$, $BL_{n-1,k}^{t}$ can be generated by $BL_{1}^{k}(N^{t}(\cdot))$, $\cdots$, $BL_{k-1}^{k}(N^{t}(\cdot))$. This leads that the dimension of $\left(BL_{i,k}^{t}\right)_{i=1,\cdots,n-1}$ is no more than $(k-1)$.

If the number of ancestral lineages is no more than k before a given standard coalescent time t, the number of inference time intervals should be no more than $(k-1)$ before time t in the inferred demographic history without overfitting. Technically speaking, if a high proportion of the number of ancestral lineages is no more than k before a given standard coalescent time t, we have the same conclusion because it is an inferred demographic history.

For the non-African populations, when $t = 1.0$, the number of ancestral lineages is no more than three in more than 90% cases (Table S18), indicating the power to infer an constant size model (with one inference time interval), an expansion or contraction (with two inference time intervals) beyond this time point. The end time of the super bottleneck is 813 (772–864) kyr ago and the corresponding standard coalescent time is larger than 1.0 for all non-African populations (Fig. 3c, 3f). Therefore, the super bottleneck cannot be inferred in this case since the bottleneck contains three inference time intervals.

Confounding factors of bottleneck

African populations have complex population structure[11-14], and a complex population structure model is proposed for African and European populations[12] (Fig. S31). To address the effects of population structure, we simulated data for a western rainforest hunter-gatherer (wRHG) and a western farmer (wARG) population and estimated their demographic histories (Fig. S31). Due to frequent migrations, a larger recent population size is estimated for both populations. However, the ancient population size (14,427) is

accurately inferred for both populations (14,493 and 14,428). Thus, the super bottleneck is not due to the complex African population structure.

To consider the effects of archaic introgression from ghost populations[15,16], we examined different models by assuming that introgression happened in different time periods with different migration rates (Fig. S32). Results show that archaic introgression does not result in an ancient super bottleneck.

Truncated SFS was used in demography inference in this study. To examine the effects of SFS truncation, the FitCoal inference was re-performed by taking the full SFSs that include high-frequency derived mutations. Again, the super bottleneck is revealed only in the African populations, but not in the non-African populations (Fig. S33, S34). Therefore, the ancient super bottleneck is not due to the effects of SFS truncation.

Computational performance

We compared the performance of the FitCoal with or without tabulation. We applied them to analyze the data of YRI population by fixing four inference time intervals and allowing instantaneous population size change. The former is much faster than the latter (1 second *vs* 36.2 hours).

Models and simulation commands for Fig. S35

We simulated trees for 10 sequences with 1,000,000 replications using the ms software[17] to calculate the average branch length for each SFS type. In this section, time is scaled by $4N_0$ generations and the population size is scaled by N_0 when using the ms software.

1. Constant size model (Fig. S35a)

The corresponding ms command is

ms 10 1000000 -L -T

2. Exponential growth model (Fig. S35b)

We assumed an ancient population size of 0.5, and the population began an exponential growth at time of 0.17328679513998632 to the current size of 1.0. The corresponding ms command is

ms 10 1000000 -G 4.0 -eN 0.17328679513998632 0.5 -L -T

3. Bottleneck model (Fig. S35c)

We assumed a population size of 1.0 and a population size of 0.5 during time of 0.1 and 0.25. The corresponding ms command is

ms 10 1000000 -eN 0.1 0.5 -eN 0.25 1.0 -L -T

4. Complex model (Fig. S35d)

We assumed an ancient population size of 0.5. The population experienced a bottleneck with population size decreasing to 0.2 from time of 0.11465735902799726 to 0.08465735902799726 and growing exponentially to the current size of 1.0. The corresponding ms command for the simulation is

ms 10 1000000 -G 20.0 -eN 0.03465735902799726 0.5 -eN 0.08465735902799726 0.2 -eN 0.11465735902799726 0.5 -L –T

Models and simulation commands for Table S15

To ensure the accuracy of FitCoal, we compared the expected branch length of FitCoal ($n = 10$) with Zivković-Wiehe's method[2] that is a numerical calculation method for piecewise constant model with at most three inference time intervals. In this section, time is scaled by $4N_0$ generations and the population size is scaled by N_0 because of the requirement of Zivković-Wiehe's method.

1. Constant size model

The corresponding input parameters of Zivković-Wiehe's method are

unfoldedfreq[10, 0.0, 0.0, 1.0, 1.0]

2. Instantaneous growth model

We assumed a current population size of 1.0 and an ancient population size of 0.5 before time 0.5. The corresponding input parameters of Zivković-Wiehe's method are

unfoldedfreq[10, 0.5, 0.0, 0.5, 0.5]

3. Bottleneck model

We assumed a population size of 1.0 and a population size of 0.5 during time of 0.1 and 0.25. The corresponding input parameters of Zivković-Wiehe's method are

unfoldedfreq[10, 0.2, 0.6, 0.5, 1]

Models for verifying the accuracy of FitCoal

If not specified, we used a default mutation rate μ of 1.2×10^{-8} per base per generation and a recombination rate $r = 0.8\mu$. All models were simulated with 200 replications using ms[17] or MaCS[18]. In this section, time is scaled by $4N_0$ generations and the population size is scaled by N_0 because of the requirement of simulation softwares.

1. Constant size model (Fig. 2a, S3a, S14a and S15a)

We assumed the effective population size of 10,000. And 30 sequences of 10 Mb were simulated. The corresponding ms command is

ms 30 200 -t 4800 -r 3800 10000000

2. Instantaneous increase model (Fig. 2b, S3b, S14b and S15b)

We used this model to mimic the demography of an African population[19]. We assumed the ancient population size of 7,778 and the current population size of 25,636 and the population began an instantaneous increase at 6,809 generations ago. 30 sequences of 10 Mb were simulated. The corresponding ms command for the simulation is

ms 30 200 -t 12310 -r 9750 10000000 -eN 0.066 0.3

3. PSMC "standard" model (Fig. 2c, S3c, S14c and S15c)

This model was based on the "standard simulation" model in PSMC publication[20]. 170 sequences of 30Mb were simulated. The corresponding MaCS command for this simulation is

macs 170 30000000 -i 200 -h 1e3 -t 0.002732 -r 0.002179 -h 1e3 -eN 0.01 0.05 -eN 0.0375 0.5 -eN 1.25 1

4. Exponential growth model I (Fig. 2d, S3d, S14d and S15d)

We assumed the current population size of 50,000 and a growth rate r = 0.004. 30 sequences of 10 Mb were simulated. The corresponding ms command for the simulation is

ms 30 200 -t 24000 -r 19000 10000000 -G 800

5. Exponential growth model II (Fig. 2e, S3e, S14e and S15e)

We used this model to mimic the demography of a European populations[21]. We assumed the ancient population size of 1,000 and the current population size of 29,525

and the population began exponential growth at 848 generations ago. 30 sequences of 10 Mb were simulated. The corresponding ms command for the simulation is

ms 30 200 -t 14172 -r 10629 10000000 -G 472.4 -eN 0.00718 0.0339

6. Exponential growth model III (Fig. 2f, S3f, S14f and S15f)

We assumed the ancient population size of 8,000. The population experienced an instantaneous decrease to 7,900 and then began exponentially growth to 900,000. 30 sequences of 10 Mb were simulated. The corresponding ms command for the simulation is

ms 30 200 -t 432000 -r 340000 10000000 -G 46368 -eN 0.0001027 0.008889

7. PSMC "sim-YH" model (Fig. S4a and S16a)

This model was based on the "sim-YH" model in the PSMC publication[20]. 170 sequences of 30 Mb were simulated. The corresponding MaCS command for the simulation is

macs 170 30000000 -i 200 -h 1e3 -t 0.002171 -r 0.001731 -eN 0.0055 0.0832 -eN 0.0089 0.0489 -eN 0.0130 0.0607 -eN 0.0177 0.1072 -eN 0.0233 0.2093 -eN 0.0299 0.3630 -eN 0.0375 0.5041 -eN 0.0465 0.5870 -eN 0.0571 0.6343 -eN 0.0695 0.6138 -eN 0.0840 0.5292 -eN 0.1010 0.4409 -eN 0.1210 0.3749 -eN 0.1444 0.3313 -eN 0.1718 0.3066 -eN 0.2040 0.2952 -eN 0.2418 0.2915 -eN 0.2860 0.2950 -eN 0.3379 0.3103 -eN 0.3988 0.3458 -eN 0.4701 0.4109 -eN 0.5538 0.5048 -eN 0.6520 0.6520 -eN 0.7671 0.6440 -eN 0.9020 0.6178 -eN 1.0603 0.5345 -eN 1.4635 1.7931

8. PSMC "sim-1" model (Fig. S4b and S16b)

This model was based on the "sim-1" model in the PSMC publication[20]. 170 sequences of 30 Mb were simulated. The corresponding MaCS command for the simulation is

macs 170 30000000 -i 200 -h 1e3 -t 0.001 -r 0.0008 -eN 0.01 0.1 -eN 0.06 1 -eN 0.2 0.5 -eN 1 1 -eN 2 2

9. PSMC "sim-2" model (Fig. S4c and S16c)

This model was based on the "sim-1" model in the PSMC publication[20]. 170 sequences of 30 Mb were simulated. The corresponding MaCS command for the simulation is

macs 170 30000000 -i 200 -h 1e3 -t 0.0001 -r 0.00008 -eN 0.1 5 -eN 0.6 20 -eN 2 5 -eN 10 10 -eN 20 5

10. PSMC "sim-3" model (Fig. S4d and S16d)

This model was based on the "sim-1" model in the PSMC publication[20]. 170 sequences of 30 Mb were simulated. The corresponding MaCS command for the simulation is

macs 170 30000000 -i 200 -h 1e3 -t 0.002 -r 0.0016 -eN 0.01 0.05 -eN 0.0150 0.5 -eN 0.05 0.25 -eN 0.5 0.5

11. Complicated model III (Fig. S4e and S16e)

We assumed the ancient population size of 4,167. The population experienced an instantaneous increase to 20,833 at 33,333 generations ago, an instantaneous decrease to 2,083 at 2,500 generations ago and an instantaneous increase to 41,667 at 833 generations ago. 170 sequences of 30 Mb were simulated. The corresponding MaCS command for the simulation is

macs 170 30000000 -i 200 -h 1e3 -t 0.002 -r 0.0016 -eN 0.005 0.05 -eN 0.0150 0.5 -eN 0.2 0.1

12. Complicated model II (Fig. S4f and S16f)

We assumed the ancient population size of 1,250. The population experienced an instantaneous increase to 33,333 at 33,333 generations ago, an instantaneous decrease to 12,500 at 16,667 generations ago, an instantaneous increase to 20,833 at 8,333 generations ago, an instantaneous decrease to 8,333 at 4,167 generations ago, an instantaneous decrease to 2,083 at 1,667 generations ago and an instantaneous increase to 41,667 at 833 generations ago. 170 sequences of 30 Mb were simulated. The corresponding MaCS command for the simulation is

macs 170 30000000 -i 200 -h 1e3 -t 0.002 -r 0.0016 -eN 0.005 0.05 -eN 0.01 0.2 -eN 0.0250 0.5 -eN 0.05 0.3 -eN 0.1 0.8 -eN 0.2 0.03

13. Exponential growth model IV (Fig. S4g and S16g)

We assumed the ancient population size of 20,000. The population experienced an instantaneous decrease to 1,000 at 4,000 generations ago, and began exponential growth to 20,000 at 2,000 generations ago. 170 sequences of 30 Mb were simulated. The corresponding MaCS command for the simulation is

macs 170 30000000 -i 200 -h 1e3 -t 0.001 -r 0.0008 -G 120 -eG 0.025 0 -eN 0.05 1

14. Exponential growth model V (Fig. S4h and S16h)

We assumed the ancient population size of 15,000. The population experienced an instantaneous decrease to 6,000 at 4,000 generations ago, and began exponential growth to 30,000 at 2,000 generations ago. 170 sequences of 30 Mb were simulated. The corresponding MaCS command for the simulation is

macs 170 30000000 -i 200 -h 1e3 -t 0.00144 -r 0.00115 -G 96.37 -eG 0.0167 0 -eN 0.033 0.5

15. Exponential growth model VI (Fig. S4i and S16i)

We assumed the ancient population size of 15,000. The population experienced an exponential decrease to 6,000 at 5,000 generations ago, and began exponential growth to 30,000 at 2,000 generations ago. 170 sequences of 30 Mb were simulated. The corresponding ms command for the simulation is

ms 170 100 -t 1440 -r 1152 1000000 -G 96.56627474604602 -eG 0.01666666666667 -36.65162927 -eN 0.0416666666667 0.5

16. Split model I (Fig. S17a)

We used this model to mimic the split demography of African hunter-gatherer and agriculturist populations. We assumed the ancient population size of 20,833. The ancient population splits into two subpopulation at 6,667 generations ago. Population 1 experienced an instantaneous increase to 41,667 at 500 generations ago, and population 2 experienced an instantaneous decline to 8,333 at 1,250 generations ago. 170 sequences of 30 Mb were simulated. The corresponding MaCS command for the simulation is

macs 340 30000000 -i 1 -h 1e3 -t 0.002 -r 0.0016 -I 2 170 170 4 -n 2 0.2 -en 0.003 1 0.5 -en 0.0075 2 0.5 -ej 0.04 2 1

17. Split model II (Fig. S17b)

We used this model to mimic the split demography of African and European populations. We assumed the ancient population size of 20,833. The ancient population split into two subpopulation at 5,000 generations ago and the population size of population 1 became 83,303. Then, population 1 experienced an instantaneous increase to 20,833 at 833 generations ago. Population 2 experienced an instantaneous increase to

41,667 at 500 generations ago. 170 sequences of 30 Mb were simulated. The corresponding MaCS command for the simulation is

macs 340 30000000 -i 1 -h 1e3 -t 0.004 -r 0.0032 -I 2 170 170 4 -n 2 0.5 -en 0.0015 2 0.25 -en 0.0025 1 0.1 -ej 0.015 1 2

18. Split model III (Fig. S17c)

We assumed the ancient population size of 4,167. The ancient population experienced an instantaneous growth to 20,833 at 8,333 generations ago and splits into two subpopulations at 2,500 generations ago. The population size of population 1 decreased to 2,083 at 1,666 generations ago and increased to 20,833 at 833 generations ago. The population size of population 2 remained constant. 170 sequences of 100 Mb were simulated. The corresponding MaCS command for the simulation is

macs 340 1000000 -i 100 -h 1e3 -t 0.001 -r 0.0008 -I 2 170 170 4 -eN 0 1 -en 0.01 1 0.1 -en 0.02 1 1 -ej 0.03 2 1 -eN 0.10 0.2 -eN 1 1

19. Models for studying influence factors of FitCoal (Fig. S2)

We simulated variations of the Exponential growth model V by increasing or decreasing the number of sequences, length of sequences and recombination rate.

19.1. Number of sequence n = 170, sequence length L = 1 Mb, recombination rate $\rho = 0.8\mu$ (Fig. S2a). The corresponding ms command for the simulation is

ms 170 1 -t 1440 -r 1152 1000000 -G 96.56627474604602 -eN 0.016666666666666666 0.2 -eN 0.03333333333333333 0.5

19.2. Number of sequence n = 170, sequence length L = 10 Mb, recombination rate $\rho = 0.8\mu$ (Fig. S2b). The corresponding ms command for the simulation is

ms 170 10 -t 1440 -r 11520 1000000 -G 96.56627474604602 -eN 0.016666666666666666 0.2 -eN 0.03333333333333333 0.5

19.3. Number of sequence n = 170, sequence length L = 100 Mb, recombination rate $\rho = 0.8\mu$ (Fig. S2c, S2f and S2h). The corresponding ms command for the simulation is

ms 170 100 -t 14400 -r 11520 10000000 -G 96.56627474604602 -eN 0.016666666666666666 0.2 -eN 0.03333333333333333 0.5

19.4. Number of sequence n = 10, sequence length L = 100 Mb, recombination rate $\rho = 0.8\mu$ (Fig. S2d). The corresponding ms command for the simulation is

ms 10 100 -t 14400 -r 11520 10000000 -G 96.56627474604602 -eN 0.016666666666666666 0.2 -eN 0.03333333333333333 0.5

19.5. Number of sequence n = 100, sequence length L = 100 Mb, recombination rate $\rho = 0.8\mu$ (Fig. S2e). The corresponding ms command for the simulation is

ms 100 100 -t 14400 -r 11520 10000000 -G 96.56627474604602 -eN 0.016666666666666666 0.2 -eN 0.03333333333333333 0.5

19.6. Number of sequence n = 170, sequence length L = 100 Mb, recombination rate $\rho = 0.1\mu$ (Fig. S2g). The corresponding ms command for the simulation is

ms 170 100 -t 14400 -r 1440 10000000 -G 96.56627474604602 -eN 0.016666666666666666 0.2 -eN 0.03333333333333333 0.5

19.7. Number of sequence n = 170, sequence length L = 100 Mb, recombination rate $\rho = 10\mu$ (Fig. S2i). The corresponding ms command for the simulation is

ms 170 100 -t 14400 -r 144000 10000000 -G 96.56627474604602 -eN 0.016666666666666666 0.2 -eN 0.03333333333333333 0.5

20. Models for studying the super bottleneck

For 1000GP, we used recent population expansion parameters of YRI and CHB to represent the recent population expansion for African and non-African population, respectively. Then, we used approximate average value of parameters inferred from African and non-African populations to represent other parameters of corresponding models.

For HGDP-CEPH, we used recent population expansion parameters of Yoruba and Han to represent the recent population expansion for African and non-African population, respectively. Then, we used approximate average value of parameters inferred from African except Biaka and non-African populations to represent other parameters of corresponding models. Because of the difference of ancient demography between Biaka and other African populations, we did not take it into consideration.

For idealized models, we fine-tuned parameters so that all parameters had a standard coalescent time smaller than 2.0.

20.1. Bottleneck I model for 1000GP (Fig. 4a and 4b)

We used this model to mimic the demography of African populations. We assumed the ancient population size of 96,000. The population experienced an instantaneous

decrease to 1,600 at 39,000 generations ago, an instantaneous growth to 27,000 at 32,500 generations ago and began exponential growth to 160,000 at 200 generations ago. 202 sequences of 800 Mb were simulated. The corresponding ms command for the simulation is

ms 202 80000 -t 76.8 -r 61.43 10000 -G 5693.878237534393 -eN 3.125E-4 0.16875 -eN 0.05078125 0.01 -eN 0.0609375 0.6

20.2. Bottleneck II model for 1000GP (Fig. 4c)

We used this model to mimic the estimated demography of non-African populations. We assumed the ancient population size of 20,000. The population experienced an exponential decrease to 6,000 at 20,000 generations ago and began exponential growth to 250,000 at 1,000 generations ago. 202 sequences of 800 Mb were simulated. The corresponding ms command for the simulation is

ms 200 80000 -t 120 -r 96 10000 -G 3729.7014486341914 -eN 0.001 0.024 -eG 0.001 -63.36698970136505 -eN 0.02 0.08

20.3. Bottleneck III model for 1000GP (Fig. 4d)

We used this model to mimic the real demography of non-African populations. We assumed the ancient population size of 96,000. The population experienced an instantaneous decrease to 1,600 at 39,000 generations ago, an instantaneous growth to 27,000 at 32,500 generations ago. Then, the population began exponential decline to 6,000 at 24,735 generations ago and instantaneously increased to 250,000 at 1,000 generations ago. 200 sequences of 800 Mb were simulated. The corresponding ms command for the simulation is

ms 200 80000 -t 120 -r 96 10000 -G 3729.7014486341914 -eN 0.001 0.024 -eG 0.001 -63.36959750479352 -eN 0.024735 0.108 -eN 0.0325 0.0064 -eN 0.039 0.384

20.4. Bottleneck IV model for HGDP-CEPH (Fig. S8a and S8b)

We used this model to mimic the demography of African populations. We assumed the ancient population size of 120,000. The population experienced an instantaneous decrease to 1,400 at 41,000 generations ago, an instantaneous growth to 28,000 at 35,000 generations ago and began instantaneous growth to 50,000 at 500 generations ago. 44 sequences of 800 Mb were simulated. The corresponding ms command for the simulation is

ms 44 80000 -t 24 -r 19.19 10000 -eN 0.0025 0.56 -eN 0.17500000000000002 0.028 -eN 0.205 2.4

20.5. Bottleneck V model for HGDP-CEPH (Fig. S8c)

We used this model to mimic the estimated demography of non-African populations. We assumed the ancient population size of 21,000. The population experienced an exponential decrease to 6,000 at 20,000 generations ago and began exponential growth to 300,000 at 1,000 generations ago. 56 sequences of 800 Mb were simulated. The corresponding ms command for the simulation is

ms 56 80000 -t 144 -r 115.19 10000 -G 4694.427606513776 -eN 8.333333333333333E-4 0.02 -eG 8.333333333333333E-4 -79.1218716944443 -eN 0.016666666666666666 0.07

20.6. Bottleneck VI model for HGDP-CEPH (Fig. S8d)

We used this model to mimic the real demography of non-African populations. We assumed the ancient population size of 120,000. The population experienced an instantaneous decrease to 1,400 at 41,000 generations ago, an instantaneous growth to 25,000 at 35,000 generations ago. Then, the population began exponential decline to 6,000 at 24,363 generations ago and instantaneously increased to 300,000 at 1,000 generations ago. 56 sequences of 800 Mb were simulated. The corresponding ms command for the simulation is

ms 56 80000 -t 144 -r 115.19 10000 -G 4694.427606513776 -eN 8.333333333333333E-4 0.02 -eG 8.333333333333333E-4 -79.12228948065652 -eN 0.0203025 0.09333333333333334 -eN 0.029166666666666667 0.004666666666666667 -eN 0.034166666666666665 0.4

20.7. Bottleneck VII model for idealized models (Fig. S9a and S9b)

We used this model to mimic the demography of African populations. We assumed the ancient population size of 30,000. The population experienced an instantaneous decrease to 3,000 at 35,000 generations ago, an instantaneous growth to 30,000 at 30,000 generations ago. 170 sequences of 800 Mb were simulated. The corresponding ms [17] command for the simulation is

ms 170 800 -t 1440 -r 1152 1000000 -eN 0.25 0.1 -eN 0.291667 1

20.8. Bottleneck VIII model for idealized models (Fig. S9c)

We used this model to mimic the estimated demography of non-African populations. We assumed the ancient population size of 20,000. The population experienced an exponential decrease to 6,000 at 20,000 generations ago and began exponential growth to 300,000 at 1,000 generations ago. 170 sequences of 800 Mb were simulated. The corresponding ms command for the simulation is

ms 170 800 -t 14400 -r 11520 1000000 -G 4694.427606513776 -eN 0.00083333 0.02 -eG 0.00083333 -101.6487102589958 -eN 0.016666666666666666 0.1

20.9. Bottleneck IX model for idealized models (Fig. S9d)

We used this model to mimic the real demography of non-African populations. We assumed the ancient population size of 30,000. The population experienced an instantaneous decrease to 3,000 at 35,000 generations ago, an instantaneous growth to 30,000 at 30,000 generations ago. Then, the population began exponential decline to 6,000 at 20,000 generations ago and instantaneously increased to 300,000 at 1,000 generations ago. 170 sequences of 800 Mb were simulated. The corresponding ms command for the simulation is

ms 170 800 -t 14400 -r 11520 1000000 -G 4694.427606513776 -eN 0.00083333 0.02 -eG 0.00083333 -101.6487102589958 -eN 0.016666666666666666 0.1 -eN 0.025 0.01 -eN 0.0291667 0.1

21. Models for estimating confidence interval

1000GP populations (Fig. S18 – S22):

ACB:

ms 192 80000 -t 37.725120000000004 -r 30.180096000000002 10000 -G 307.97400639367373 -eN 0.0033742698361377437 0.35374201592996923 -eN 0.10237507717670723 0.012990813548107999 -eN 0.1132253281877044 0.9123469984986132

ASW:

ms 122 80000 -t 26.50224 -r 21.201792 10000 -G 56.10026737541272 -eN 0.01390929179691329 0.4582616412801333 -eN 0.1538498233982067 0.013891655950591346 -eN 0.16560167778269375 1.3718870555847353

BEB:

691 ms 172 80000 -t 62.65536 -r 50.124288 10000 -G 1215.8971532452542 -eN
692 0.0023403111314833293 0.058100695614868386 -eG 0.0023403111314833293 -
693 30.907477873075123 -eN 0.03371108514231231 0.15320381209205405
694 CDX:
695 ms 186 80000 -t 25.248 -r 20.1984 10000 -G 495.40037108442965 -eN
696 0.004604646549934852 0.10216730038022814 -eG 0.004604646549934852 -
697 17.489419084798488 -eN 0.0835118490009135 0.4061216730038023
698 CEU:
699 ms 198 80000 -t 76.50768000000001 -r 61.206144 10000 -G 3486.9981711123683 -eN
700 8.189396733027973E-4 0.057518931432765964 -eN 0.01896877424771246
701 0.1280749854132291
702 CHB:
703 ms 206 80000 -t 148.45488 -r 118.763904 10000 -G 7477.99792685936 -eN
704 5.168378866508531E-4 0.020964753735276336 -eN 0.006336402867008054
705 0.06404208470614102
706 CHS:
707 ms 210 80000 -t 87.9024 -r 70.32192 10000 -G 4112.853998070424 -eN
708 8.149360963103421E-4 0.03502429967782449 -eN 0.011161187141954527
709 0.1114290394801507
710 CLM:
711 ms 188 80000 -t 26.05104 -r 20.840832 10000 -eN 0.006899708256449607
712 0.17470933981906286 -eN 0.04654813479653858 0.35472518563558303
713 ESN:
714 ms 198 80000 -t 32.99376 -r 26.395008 10000 -G 1399.7970544542743 -eN
715 6.732730258474137E-4 0.38967368375110933 -eN 0.11907424073256923
716 0.025241136505812008 -eN 0.14645778743979765 1.6907342479305179
717 FIN:
718 ms 198 80000 -t 21.88368 -r 17.506944 10000 -G 1545.9307685858762 -eN
719 0.0010069648928517855 0.21083108508258208 -eN 0.079627651288076
720 0.4667149218047421
721 GBR:

ms 182 80000 -t 68.96448 -r 55.171584 10000 -G 4780.2465803320365 -eN
4.8660205464359964E-4 0.09767810907876055 -eG 4.8660205464359964E-4
299.83121839376906 -eN 0.0026469357311387233 0.051108048665051926 -eG
0.0026469357311387233 -38.53061553796807 -eN 0.02777287031733699
0.1345666638826248
GIH:
ms 206 80000 -t 22.5384 -r 18.03072 10000 -G 319.3657263289911 -eN
0.005331789062104143 0.18217442231924183 -eG 0.005331789062104143 -
7.108545561599834 -eN 0.1312801904940001 0.4459801938025769
GWD:
ms 226 80000 -t 71.53488 -r 57.227904 10000 -G 2480.4594823364796 -eN
6.955466408858352E-4 0.17812401446678877 -eN 0.055221144353749266
0.008796827505686736 -eN 0.06446476441787029 0.7480725486643718
IBS:
ms 214 80000 -t 101.40288 -r 81.122304 10000 -G 3879.3899843730937 -eN
7.379412692860351E-4 0.05711080395349718 -eN 0.001639355380662806
0.03441322376642557 -eG 0.001639355380662806 -55.51532072601329 -eN
0.019312961005874058 0.09179857613511569
ITU:
ms 204 80000 -t 45.81072 -r 36.648576 10000 -G 942.7096023053382 -eN
0.002494089782323459 0.09525456050461552 -eN 0.026664885830212617
0.2086358826056434
JPT:
ms 208 80000 -t 55.95024 -r 44.760192 10000 -G 3128.7376262633884 -eN
8.114087494514677E-4 0.07897017063733774 -eN 0.002182047525463559
0.04600945411494213 -eG 0.002182047525463559 -42.38616087573135 -eN
0.03372169017138904 0.17515849797963332
KHV:
ms 198 80000 -t 57.9072 -r 46.32576 10000 -G 1588.3658354039515 -eN
0.0019264561851523535 0.04689157824933687 -eG 0.0019264561851523535 -
36.60290382061524 -eN 0.03792001517437307 0.17509118037135277

LWK:

ms 198 80000 -t 21.33888 -r 17.071104000000002 10000 -G 34.458048510849686 -eN 0.014319371341156495 0.6105362605722512 -eN 0.18803659662764166 0.02145942055065683 -eN 0.20879409785416014 2.0908763721432426

MSL:

ms 170 80000 -t 21.25872 -r 17.006976 10000 -G 127.20491855898698 -eN 0.003279354257615819 0.6589220799747115 -eN 0.18195660752091394 0.04585788796315112 -eN 0.23579811421655142 2.9051457472510105

MXL:

ms 128 80000 -t 72.2232 -r 57.77856 10000 -G 1185.9983336956855 -eN 0.0025552519587115612 0.04829030006978367 -eG 0.0025552519587115612 -35.997766981810344 -eN 0.030770096213141897 0.13333997939720202

PEL:

ms 170 80000 -t 104.52432 -r 83.619456 10000 -G 2449.33558491349 -eN 0.0014410414433505075 0.029316813541575778 -eN 0.01066574560965878 0.09490308092891683

PJL:

ms 192 80000 -t 40.10544 -r 32.084352 10000 -G 658.1508823918153 -eN 0.0035165490125809392 0.09882350125070315 -eG 0.0035165490125809392 -14.935034208218648 -eN 0.06458715193043525 0.2460234821011813

PUR:

ms 208 80000 -t 23.60832 -r 18.886656 10000 -eN 0.0038497802945414656 0.6750365972674041 -eN 0.014388104698224359 0.1546437865972674 -eG 0.014388104698224359 -15.582101828279491 -eN 0.07286054886643582 0.3846169486011711

STU:

ms 204 80000 -t 34.572 -r 27.657600000000002 10000 -G 510.43071934664556 -eN 0.004267252624293807 0.11325234293648039 -eN 0.02525451461678291 0.2616869142658799

TSI:

ms 214 80000 -t 75.82608 -r 60.660864000000004 10000 -G 2569.467980386571 -eN 0.0011371059177742527 0.05383899576504548 -eG 0.0011371059177742527 -19.704497360903815 -eN 0.04986270865479367 0.14062707712175018

YRI:

ms 216 80000 -t 64.91088 -r 51.928704 10000 -G 4776.570655987927 -eN 3.3888995289779744E-4 0.19814983250881826 -eN 0.0625962626099122 0.007882807936050167 -eN 0.06835272805758985 0.4330589879539455

HGDP-CEPH populations (Fig. S23 – S28):

Adygei:

ms 32 80000 -t 19.19712 -r 15.357696 10000 -eN 0.005250411630207267 0.19837975696354454 -eG 0.005250411630207267 -8.596593090355556 -eN 0.11548669953457971 0.5117517627644147

Balochi:

ms 48 80000 -t 50.949600000000004 -r 40.75968 10000 -G 623.264941916954 -eN 0.004223024540924805 0.0719299072024118 -eG 0.004223024540924805 -32.99343443398211 -eN 0.032825823542035906 0.18482264826416694

Basque:

ms 46 80000 -t 26.153760000000002 -r 20.923008 10000 -G 751.4700408942055 -eN 0.0025016313707249523 0.15260520858186355 -eG 0.0025016313707249523 -8.224106050612061 -eN 0.1199670757097625 0.40097637968689775

Bedouin:

ms 92 80000 -t 36.622080000000004 -r 29.297664 10000 -G 244.38587570241546 -eN 0.008841200644961786 0.11524850581944007 -eG 0.008841200644961786 -16.31003863953942 -eN 0.05738997874929217 0.2544039005976722

Biaka:

ms 44 80000 -t 4.5912 -r 3.6729600000000002 10000 -eN 0.009592435429723692 3.6935703084161005 -eN 0.9319760745921495 0.09492943021432305 -eG 0.9319760745921495 -11.520947944349727 -eN 1.3098356260554107 7.379299529534762

Brahui:

ms 50 80000 -t 36.26112 -r 29.008896 10000 -G 372.4275509762127 -eN
0.006063547988128193 0.10453510536905644 -eG 0.006063547988128193 -
20.411278092113488 -eN 0.05182198032003567 0.26600391824632
Burusho:
ms 48 80000 -t 11.5464 -r 9.23712 10000 -eN 0.015366836965198416
0.29627935980045733 -eG 0.015366836965198416 -8.16350928074288 -eN
0.1408168183093884 0.8250259821242986
Druze:
ms 84 80000 -t 16.18944 -r 12.951552 10000 -G 109.07256817628162 -eN
0.01288215226934864 0.24534511385199242 -eG 0.01288215226934864 -
7.35809820577746 -eN 0.13234063031350007 0.5909037001897534
French:
ms 56 80000 -t 79.18416 -r 63.347328000000005 10000 -G 2198.9359820452387 -eN
0.001348902384433904 0.051501209332775646 -eG 0.001348902384433904 -
24.36290322377743 -eN 0.03939915284814332 0.13014117975110173
Han:
ms 86 80000 -t 159.24816 -r 127.398528 10000 -G 5363.756025025552 -eN
7.370989032405503E-4 0.0191851510246649 -eN 0.005252449909354633
0.05743488653181299
Hazara:
ms 38 80000 -t 12.69792 -r 10.158336 10000 -eN 0.014217614003750299
0.25629394420503515 -eG 0.014217614003750299 -9.884907873225844 -eN
0.12245692270731047 0.7471459892643834
Japanese:
ms 54 80000 -t 33.88464 -r 27.107712 10000 -G 636.5261153273832 -eN
0.004000435354218995 0.07836471038204922 -eG 0.004000435354218995 -
26.629980477176918 -eN 0.0528258276856906 0.2876064198999901
Kalash:
ms 44 80000 -t 3.04608 -r 2.436864 10000 -G -2.415743522809092 -eN
0.47028502523586235 3.1145603529782537
Makrani:

ms 50 80000 -t 24.11088 -r 19.288704 10000 -eN 0.00980388240380426
0.14526885787661006 -eG 0.00980388240380426 -17.111271203295853 -eN
0.06723955104118398 0.388146761959746
Mandenka:
ms 44 80000 -t 13.10688 -r 10.485504 10000 -eN 0.3296277261231593
0.048304401962938545 -eG 0.3296277261231593 -17.85185708722175 -eN
0.5825077171252933 4.411191679484362
Maya:
ms 42 80000 -t 16.673280000000002 -r 13.338624000000001 10000 -eN
0.008589230112361738 0.09687356057116536 -eG 0.008589230112361738 -
25.14802627151756 -eN 0.08111110798113147 0.600155458314141
Mozabite:
ms 54 80000 -t 17.42304 -r 13.938432 10000 -G 34.034495761040134 -eN
0.03302787085100088 0.32494903300457323 -eG 0.03302787085100088 -
4.504618045303915 -eN 0.1472698871889101 0.543638767976197
Palestinian:
ms 92 80000 -t 22.33968 -r 17.871744 10000 -eN 0.008844463035145432
0.1913151844610129 -eG 0.008844463035145432 -7.866119095624621 -eN
0.11128708520369861 0.4282675490427795
Pathan:
ms 48 80000 -t 42.96432 -r 34.371456 10000 -G 497.59849646988573 -eN
0.005312881946315924 0.07109899563172419 -eG 0.005312881946315924 -
47.5703288285576 -eN 0.02861662601453915 0.21543085052899708
Russian:
ms 50 80000 -t 22.14048 -r 17.712384 10000 -G 258.609263568537 -eN
0.006473721471777433 0.1874647704114816 -eN 0.047392730886604
0.4300394571391406
Sardinian:
ms 56 80000 -t 19.90512 -r 15.924096 10000 -G 209.67966756103402 -eN
0.008361464215634221 0.17321372591574427 -eG 0.008361464215634221 -
11.622404927783043 -eN 0.09674763618341507 0.48385541006535

Sindhi:

ms 48 80000 -t 28.07088 -r 22.456704000000002 10000 -eN 0.006697787857121225 0.12812708401019132 -eG 0.006697787857121225 -17.75301871013936 -eN 0.06131324436460199 0.33785331988167094

Yakut:

ms 50 80000 -t 10.99008 -r 8.792064 10000 -G 107.01050381191519 -eN 0.010397096462590117 0.32870370370370366 -eN 0.09403222060369128 0.8740391334730957

Yoruba:

ms 44 80000 -t 30.6816 -r 24.54528 10000 -G 298.1592873494309 -eN 0.0028204398926000218 0.4313047559449311 -eN 0.1396195363438095 0.026126408010012515 -eN 0.16980043486634022 2.1113579474342927

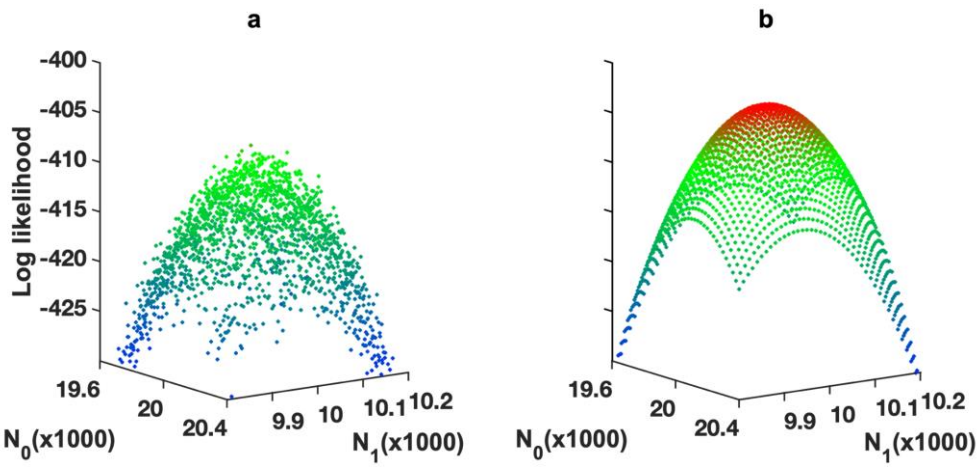

Figure S1. Comparison of likelihood surfaces based on simulations and FitCoal. (a) Likelihood surface of a SFS based on simulation approach. (b) Likelihood surface of the SFS based on FitCoal. The sample size is 100. The SFS is obtained under a demography that the population size increases from 10,000 to 20,000 at standard coalescent time 0.2. The surfaces were obtained conditional on standard coalescent time 0.2 while the current (N_0) and the ancestral population size (N_1) varied in the instantaneous growth model. Red dots indicate large likelihoods, and blue dots indicate small likelihoods.

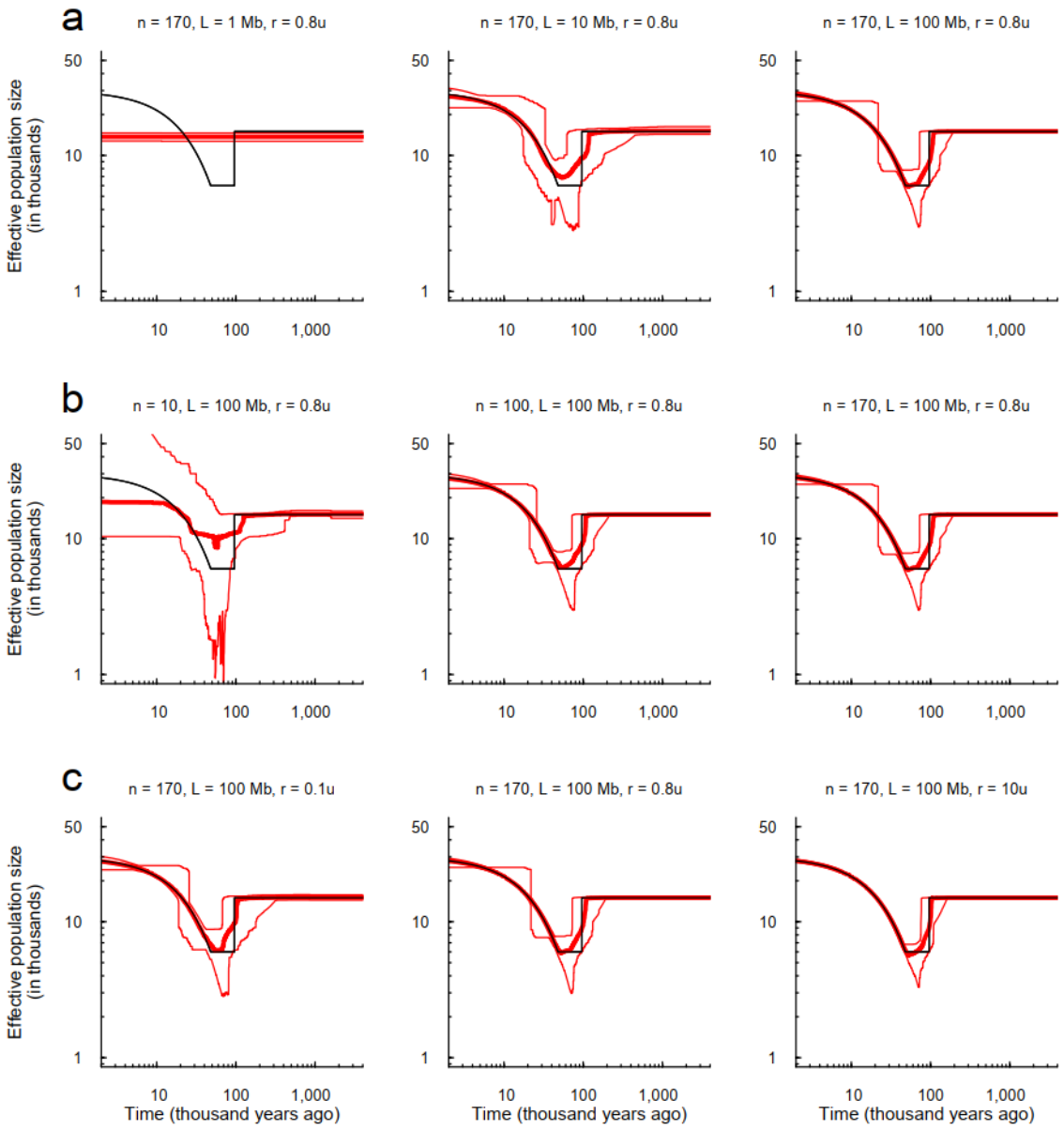

Figure S2. Effects of sequence length (a), sample size (b), and recombination rate (c) in the FitCoal inference. Thin black lines indicate true models. Thick red lines are the medians of the estimated histories of FitCoal; thin red lines are 2.5 and 97.5 percentiles of the estimated histories of FitCoal. *n* is the number of simulated sequences, *L* the length of the simulated sequences, and *r* the recombination rate relative to the mutation rate (μ). Other parameters are the same with Figure 2. The corresponding commands for simulations are described above.

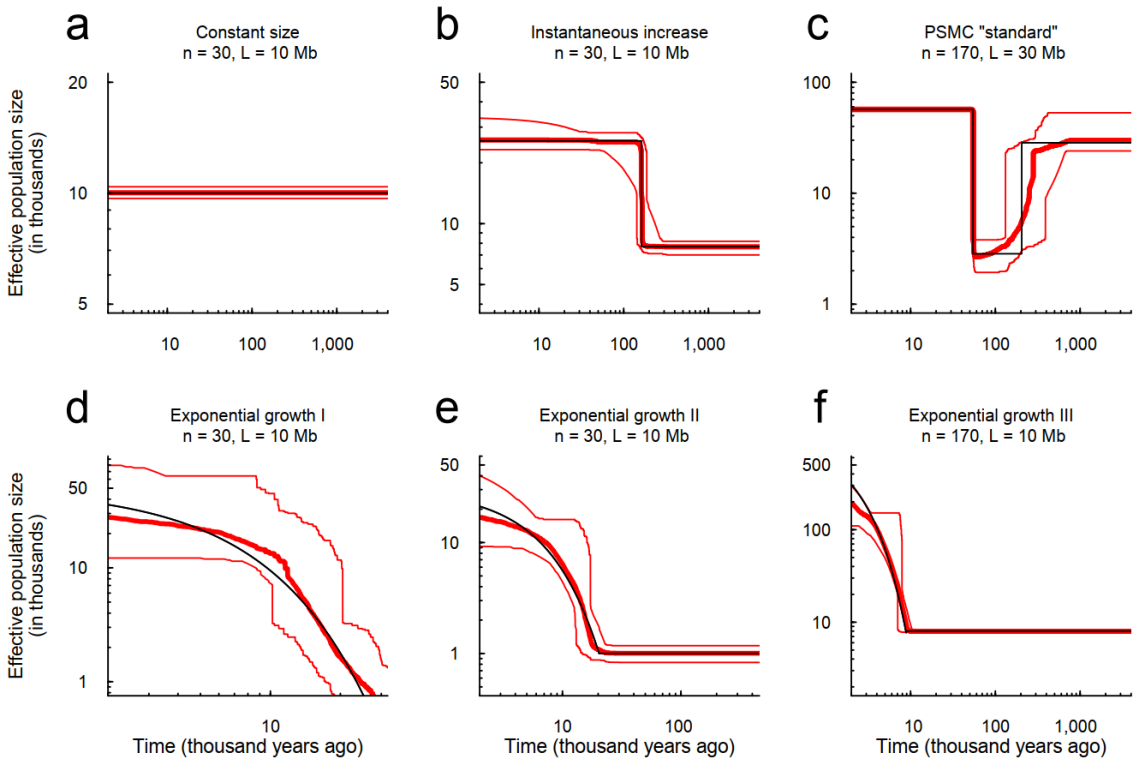

Figure S3. Verification of FitCoal accuracy with truncated SFS. (a) Constant size model. (b) Instantaneous increase model. (c) PSMC "standard" model. (d) Exponential growth I model. (e) Exponential growth II model. (f) Exponential growth III model. The six models are the same as Figure 2. Thin solid black lines indicate true models. Thick red lines are the medians of the estimated histories of FitCoal; thin red lines are 2.5 and 97.5 percentiles of the estimated histories of FitCoal. *n* is the number of simulated sequences and *L* the length of the simulated sequences. 10% SFS types (high frequency mutations) were discarded. The corresponding commands for simulations are described above.

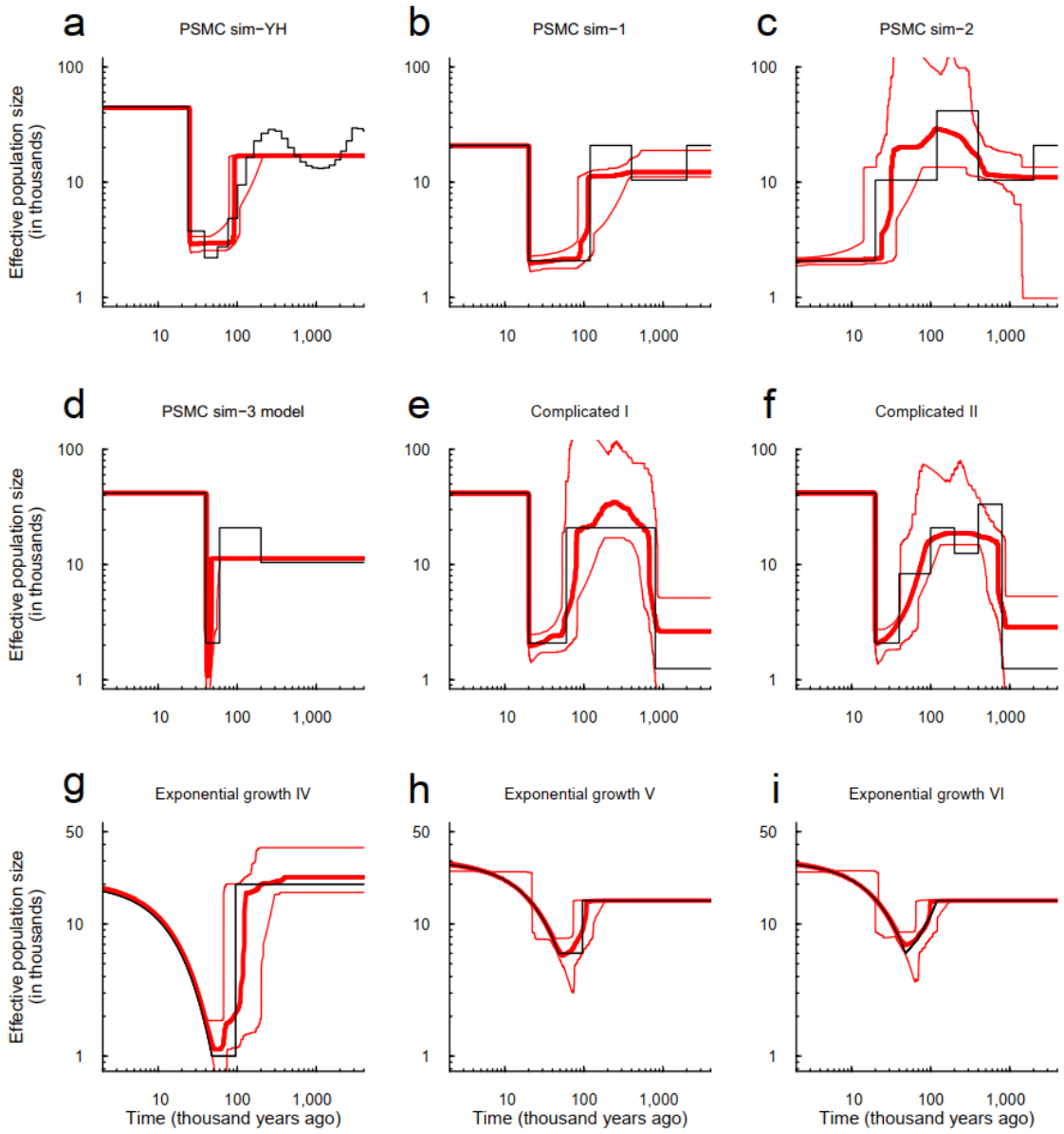

Figure S4. Verification of FitCoal accuracy with truncated SFS under more complexed models. (a) PSMC sim-YH model. (b) PSMC sim-1 model. (c) PSMC sim-2 model. (d) PSMC sim-3 model. (e) Four stage model. (f) Intricate model. (g) Exponential growth IV model. (h) Exponential growth V model. (i) Exponential growth VI model. The nine models are the same as Figure S4. Thin solid black lines indicate true models. Thick red lines are the medians of the estimated histories of FitCoal; thin red lines are 2.5 and 97.5 percentiles of the estimated histories of FitCoal. The number of simulated sequences is 170 and the length of the simulated sequences is100Mb. The corresponding commands for simulations are described above.

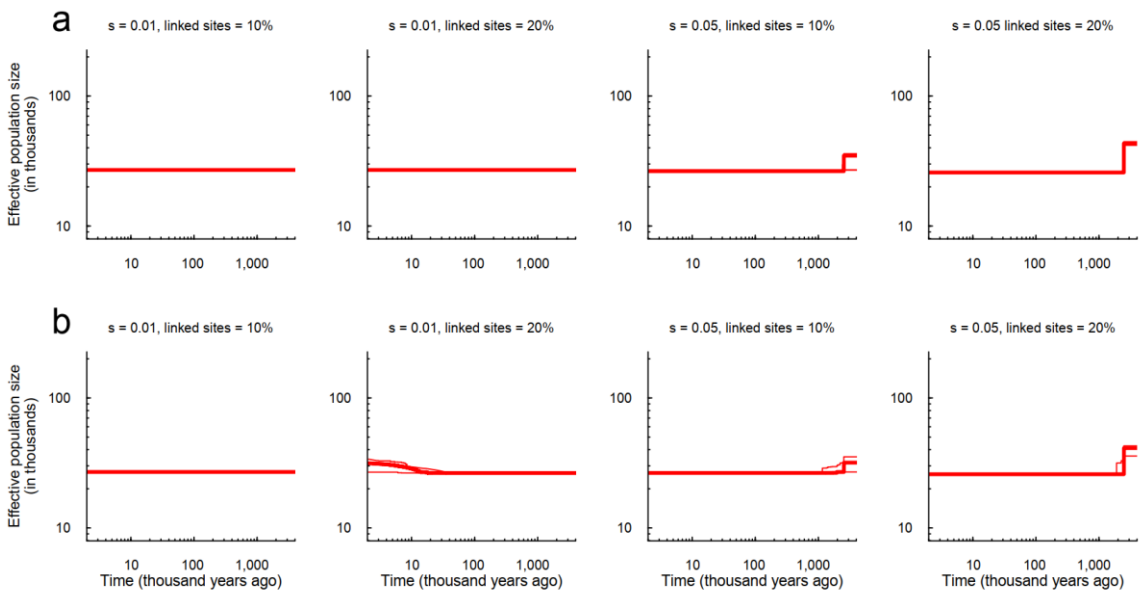

Figure S5. Effects of positive selection on demographic inference. (a) Demographic histories inferred by using the full size SFSs. (b) Demographic histories inferred by using the truncated SFSs. The constant size model was considered with different selection strength (s) and the percentage of loci affected by positive selection. $n = 202$. Thick red lines are the medians of the estimated histories of FitCoal; thin red lines are 2.5 and 97.5 percentiles of the estimated histories of FitCoal.

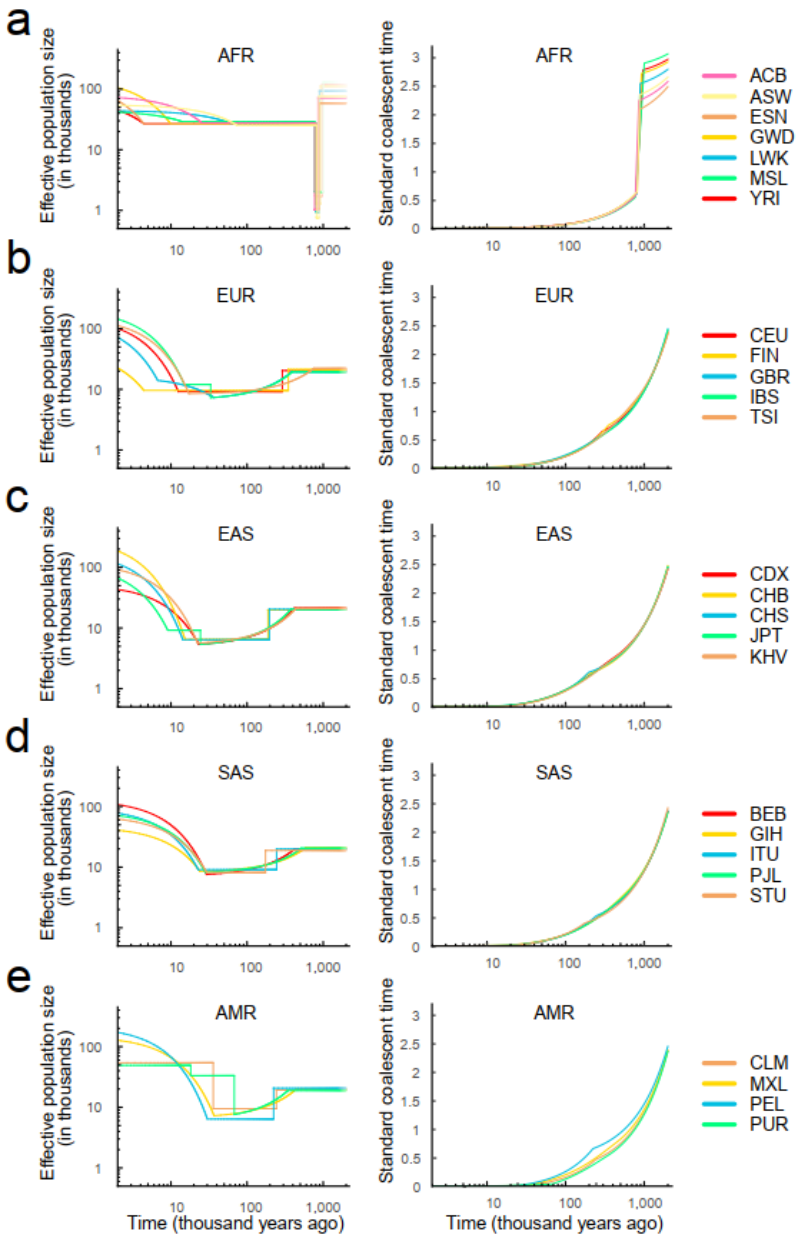

Figure S6. Inferred demographic histories and standard coalescent times of 1000GP populations. (a) African populations. (b) European populations. (c) East Asian populations. (d) South Asian populations. (e) American populations. The left column is the inferred demographic histories, and the right column is calendar time *vs* standard coalescent time. The results are the same with Figure 3.

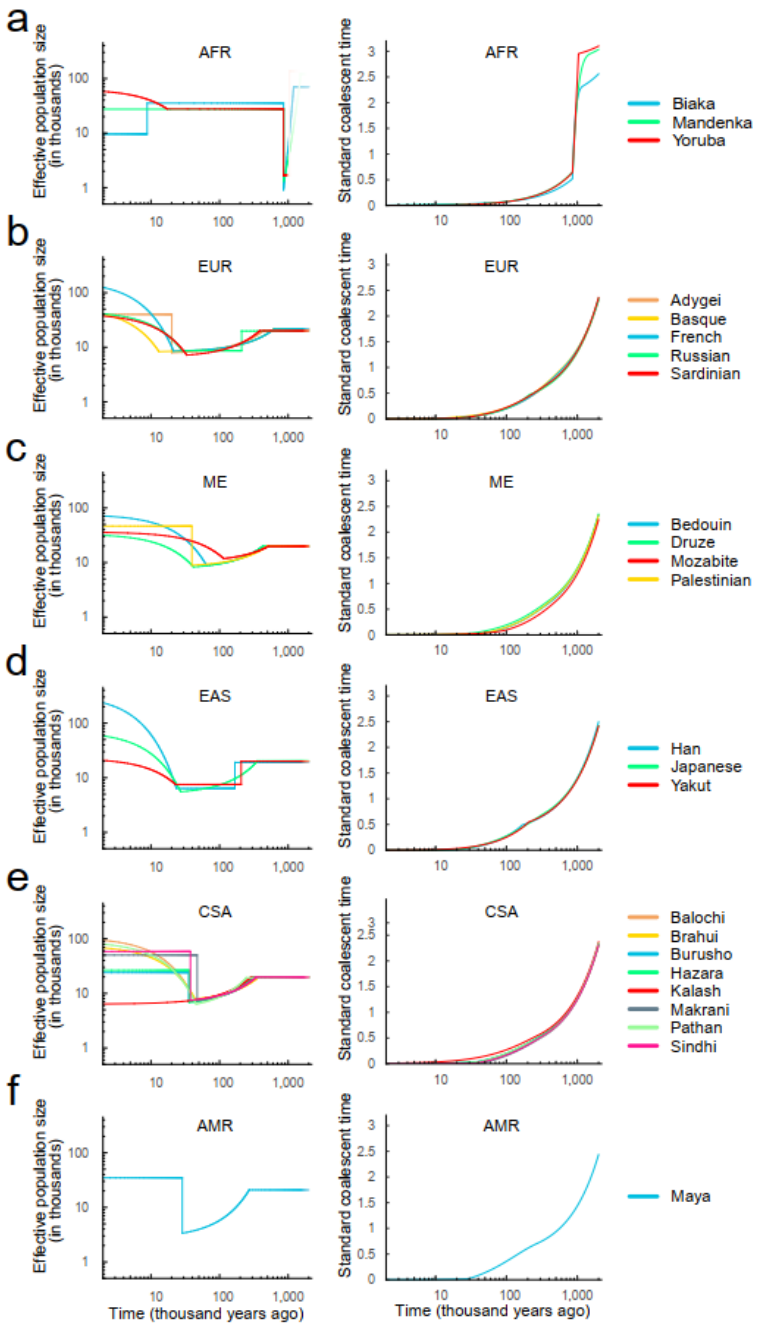

945

946 **Figure S7. Inferred demographic histories and standard coalescent times of HGPD-**
947 **CEPH populations.** (a) African populations. (b) European populations. (c) Middle East
948 populations. (d) East Asian populations. (f) Central & South Asian populations. (g)
949 American population. The left column is the inferred demographic histories, and the right
950 column is calendar time *vs* standard coalescent time. The results are the same with Figure
951 3.

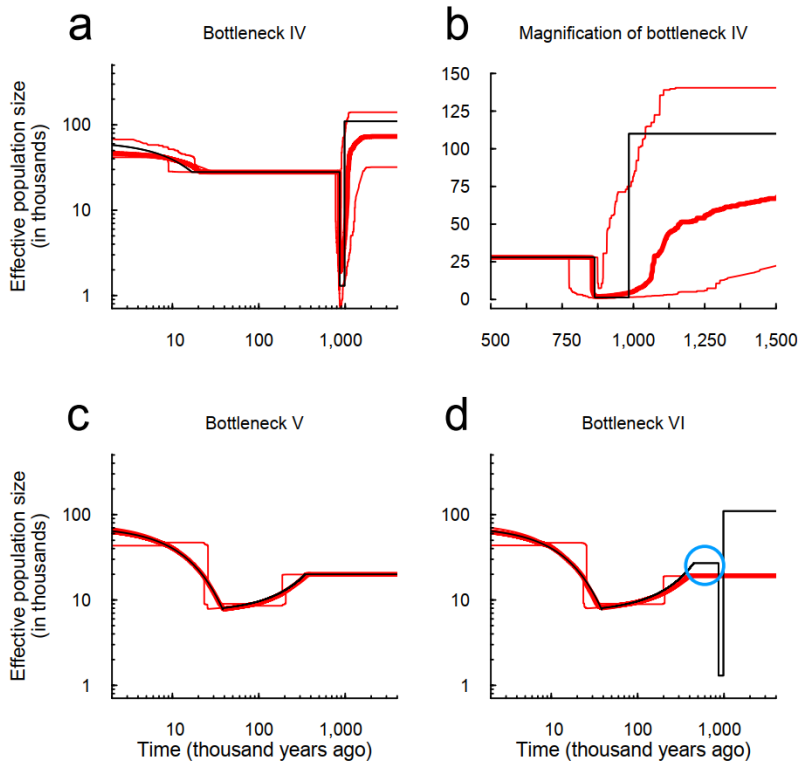

Figure S8. Verification of the HGDP-CEPH inferred super bottleneck. (a) Bottleneck IV model and the estimated histories. The bottleneck IV mimics the estimated demography of HGDP-CEPH African population. (b) Linear-scaled Bottleneck IV model during the super bottleneck. (c) Bottleneck V model and the estimated histories. The bottleneck V mimics the estimated demography of HGDP-CEPH non-African population. (d) Bottleneck VI model and the estimated histories. The bottleneck VI mimics the true demography of HGDP-CEPH non-African population. Thin black lines indicate three models. Thick red lines are the medians of the estimated histories of FitCoal; thin red lines are 2.5 and 97.5 percentiles of the estimated histories of FitCoal. Blue circle indicates the population size gap. The number of simulated sequences is 44 in Bottleneck IV, and 56 in Bottleneck V and VI, as the average sampled sequences in the HGDP-CEPH African and non-African populations. The length of simulated sequences is 800 Mb.

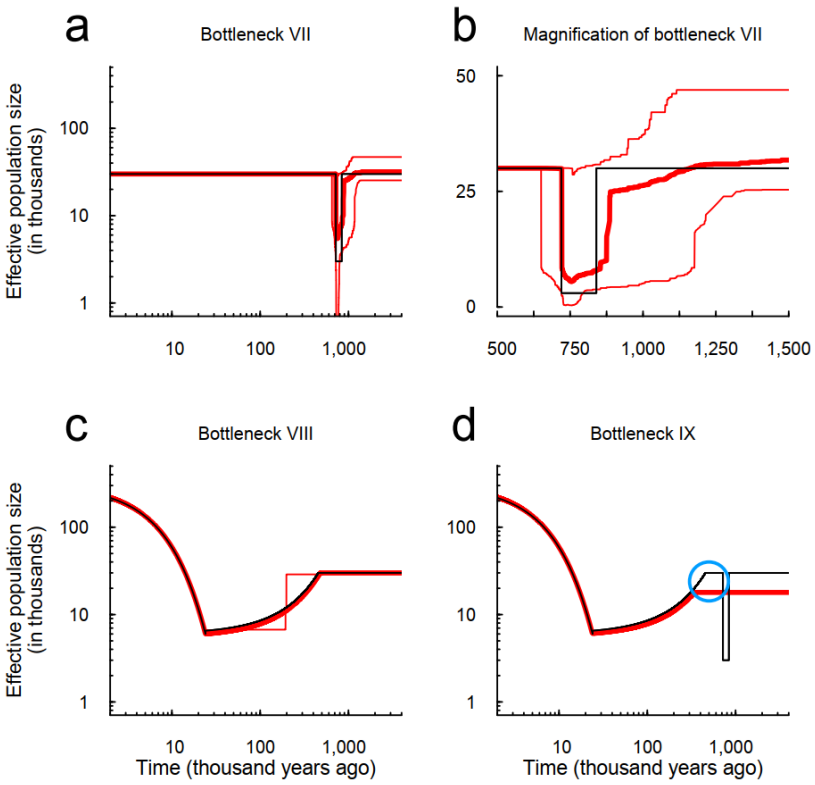

966

967 **Figure S9. Verification of the super bottleneck in artificial models.** (a) Bottleneck VII
968 model and the estimated histories. The artificial bottleneck VII represents the authors-
969 altered demography of African population. (b) Linear-scaled Bottleneck VII model
970 during the super bottleneck. (c) Bottleneck VIII model and the estimated histories. The
971 artificial bottleneck VIII represents the authors-altered estimated demography of non-
972 African population. (d) Bottleneck IX model and the estimated histories. The bottleneck
973 IX represents the authors-altered true demography of non-African population. Thin black
974 lines indicate models. Thick red lines are the medians of the estimated histories of
975 FitCoal; thin red lines are 2.5 and 97.5 percentiles of the estimated histories of FitCoal.
976 Blue circle indicates the population size gap. The number of simulated sequences is 170,
977 and the length of simulated sequences is 800 Mb.

978

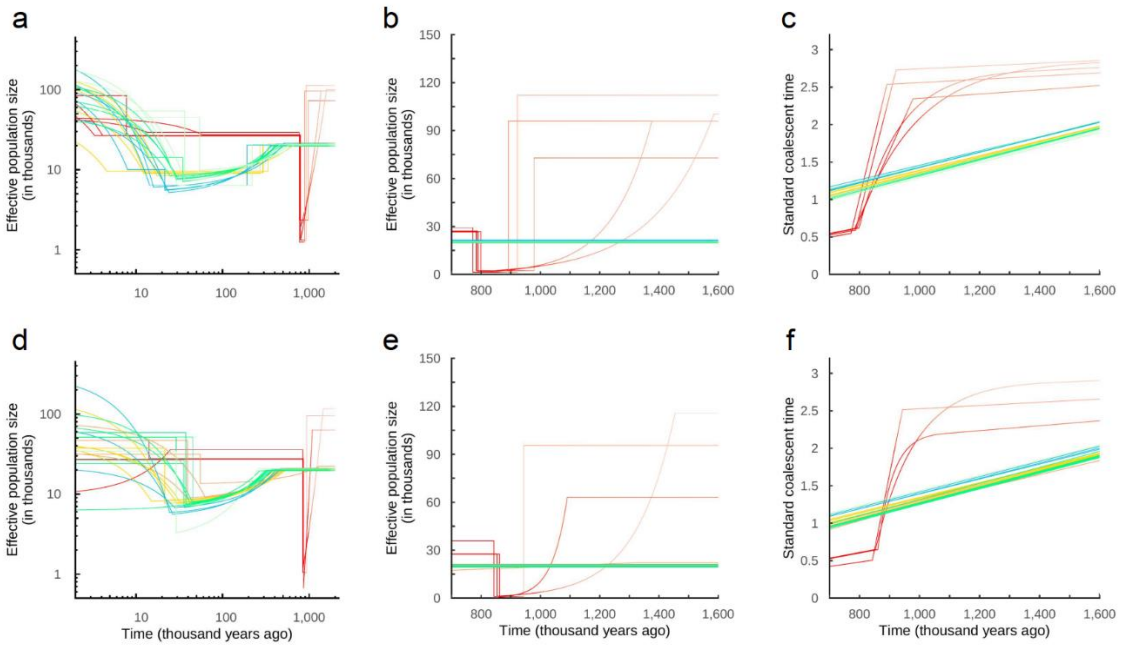

Figure S10. Inferred demographic histories of 1000GP and HGPD-CEPH populations using the same truncating SFS standard for each data set. (a) Estimated histories of 26 1000GP populations. (b) Linear-scaled estimated histories of 1000GP populations during the super bottleneck. (c) Calendar time *vs* standard coalescent time conditional on the estimated histories of 1000GP populations. (d) Estimated histories of 24 HGPD-CEPH populations. (e) Linear-scaled estimated histories of HGPD-CEPH populations during the super bottleneck. (f) Calendar time *vs* standard coalescent time conditional on the estimated histories of HGPD-CEPH populations. Red lines are the estimated histories of African populations; yellow lines stand for the European populations; brown lines the Middle East populations; blue lines the East Asian populations; green lines the Central or South Asian populations; dark sea green lines the American populations. We truncated 10% SFS types for 1000GP populations, and 15% for HGDP-CEPH populations. We assumed a mutation rate of 1.2×10^{-8} per base per generation and a generation time of 24 years, the same as Figure 2.

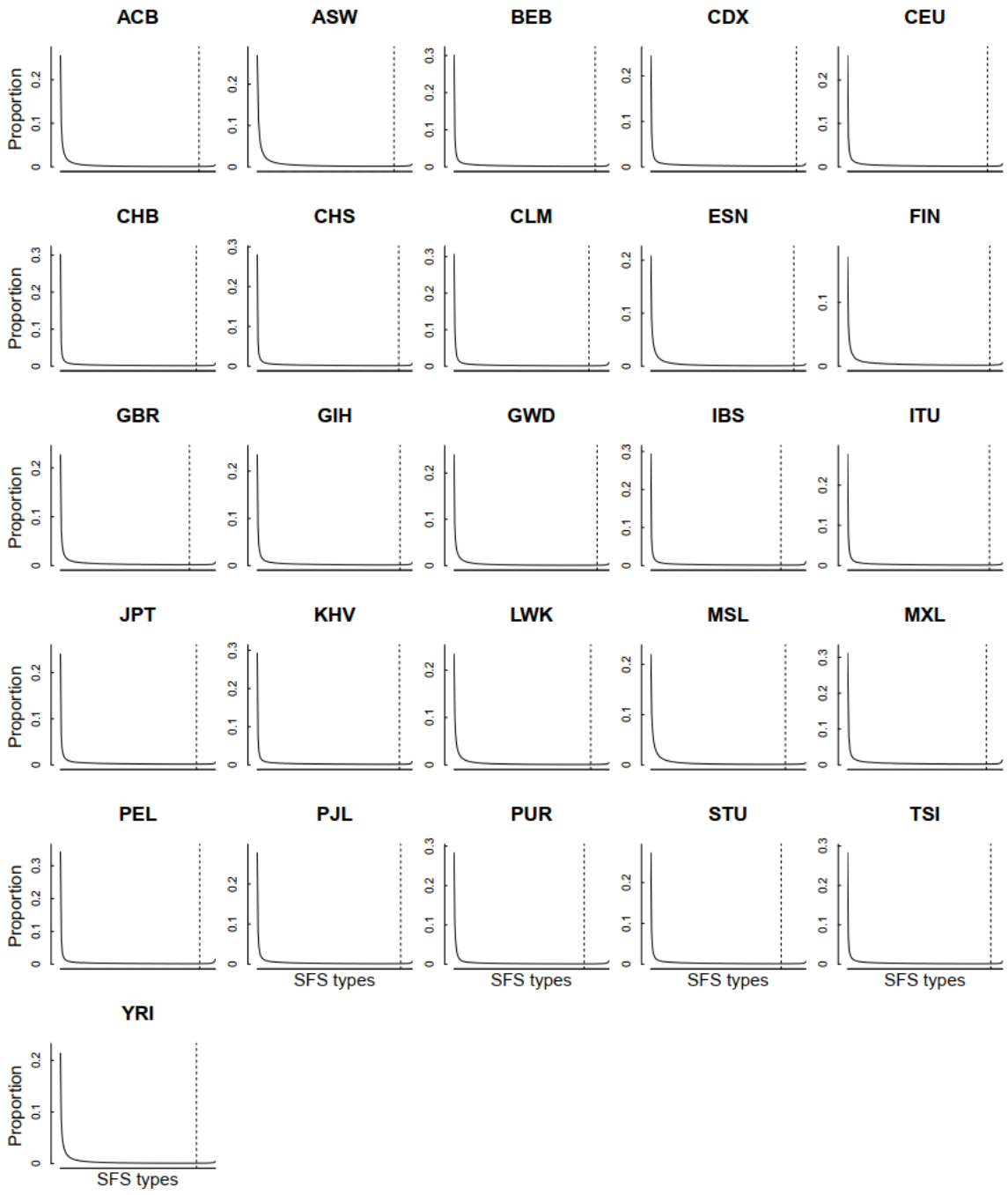

Figure S11. The observed SFSs of 1000GP populations. Solid lines indicate the observed SFS, and the *x*-axis is the SFS types, ranging from 1 to $(n-1)$. Dash lines indicate the threshold of truncating SFS.

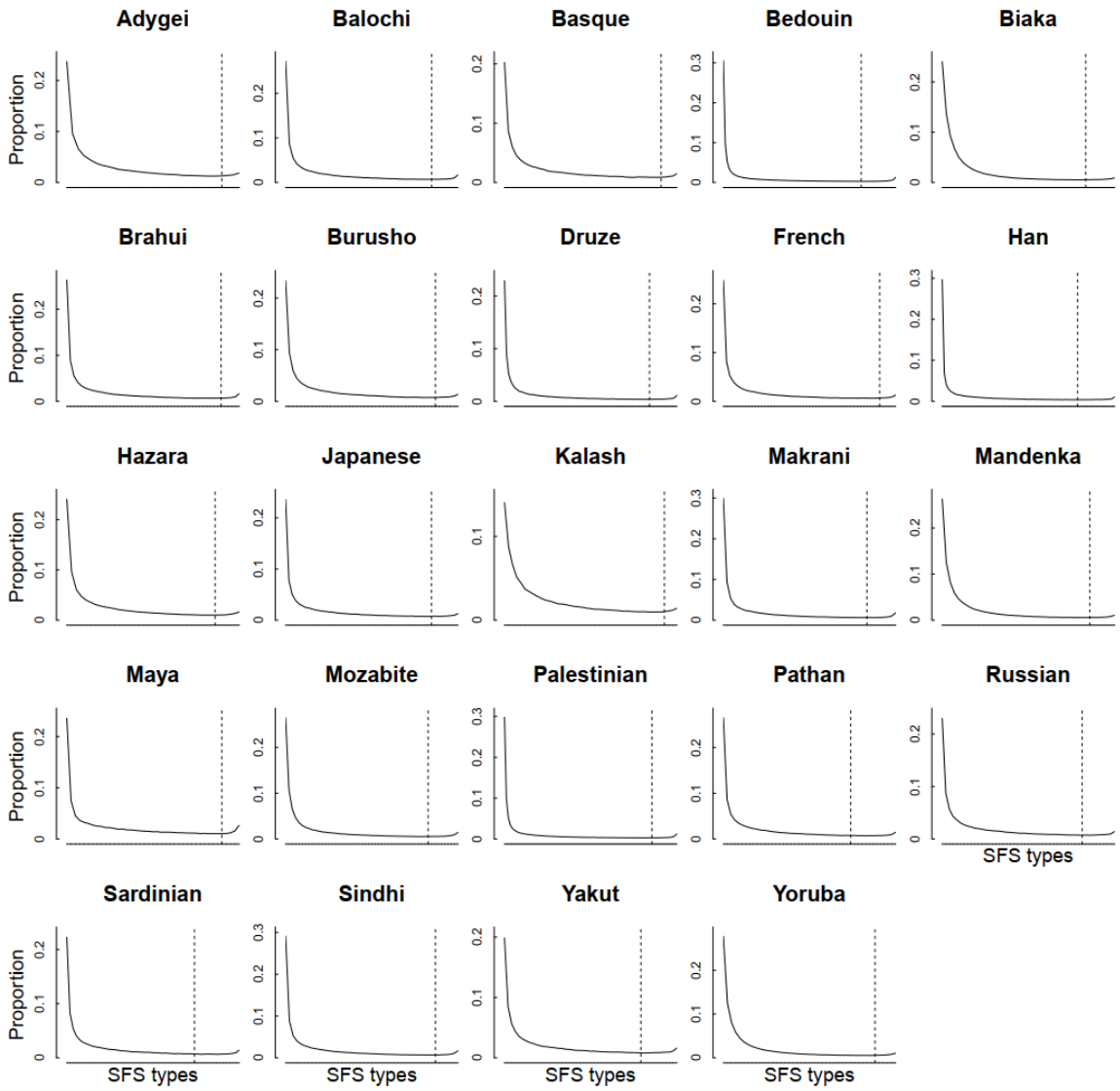

Figure S12. The observed SFSs without missing data of HGDP-CEPH populations. Solid lines indicate the observed SFS, and the *x*-axis is the SFS types, ranging from 1 to $(n-1)$. Dash lines indicate the threshold of truncating SFS.

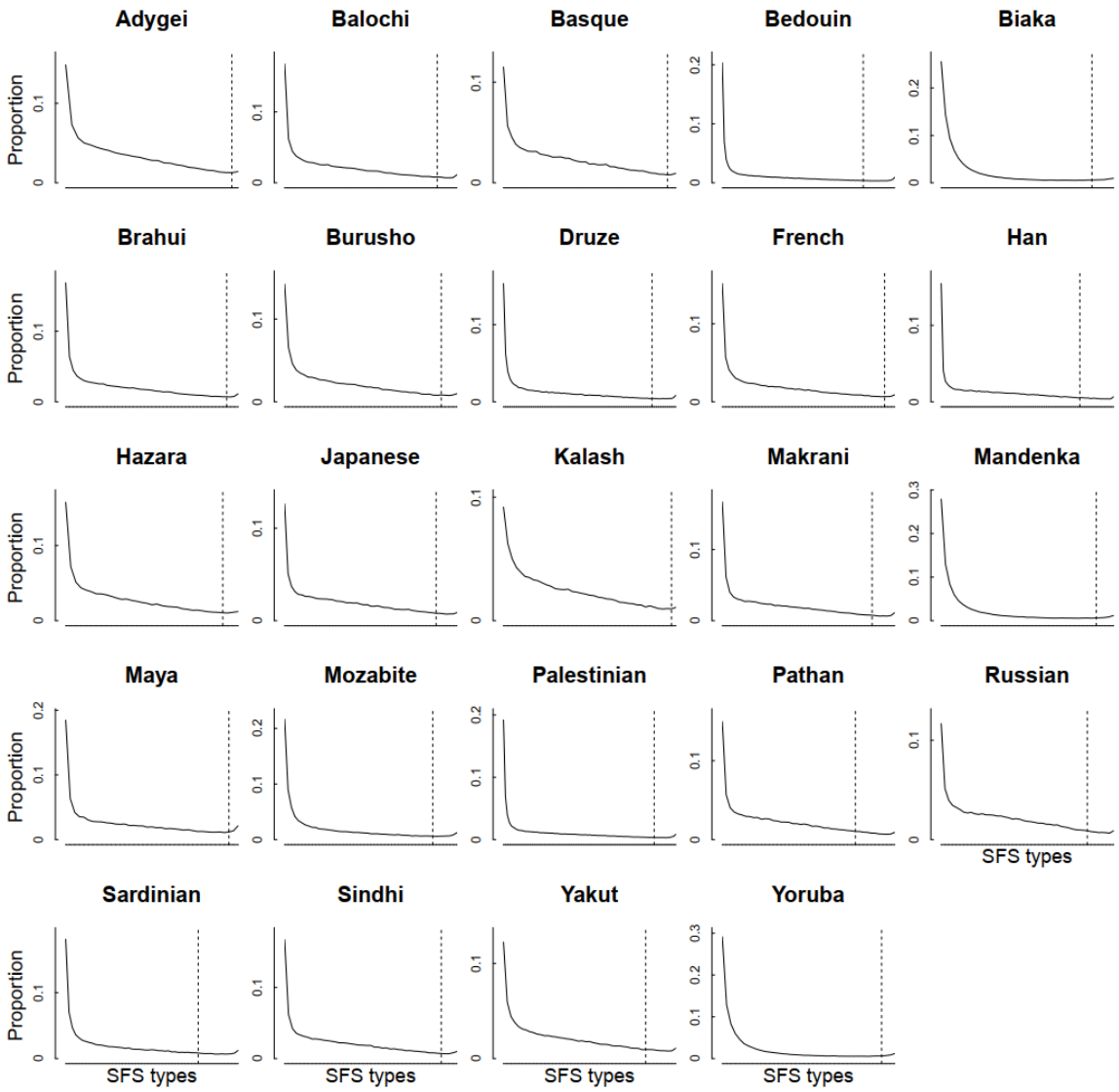

Figure S13. The observed SFSs with one missing individual of HGDP-CEPH populations. Solid lines indicate the observed SFS, and the *x*-axis is the SFS types, ranging from 1 to $(n-3)$. Dash lines indicate the threshold of truncating SFS.

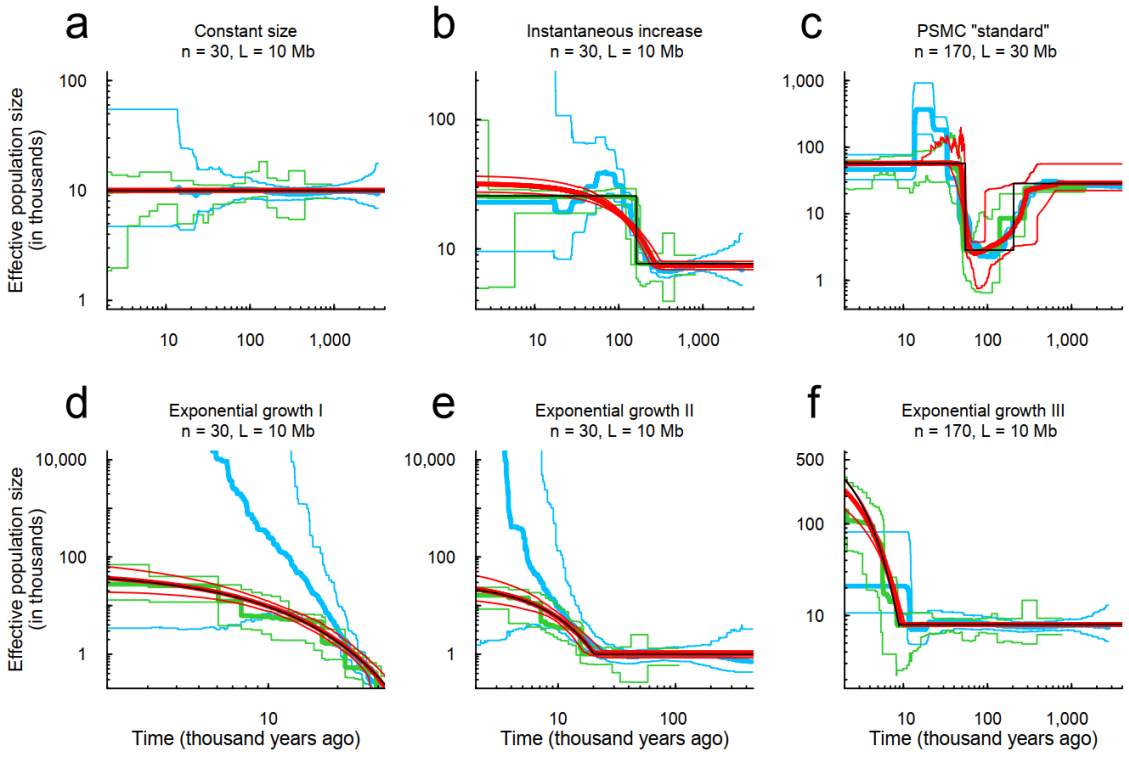

Figure S14. Estimated demographic histories of FitCoal conditional on exponential change, stairway plot, and PSMC using simulated samples. (a) Constant size model. (b) Instantaneous increase model. (c) PSMC "standard" model. (d) Exponential growth I model. (e) Exponential growth II model. (f) Exponential growth III model. Thin black lines indicate true models. Thick red lines are the medians of FitCoal histories estimated conditional on exponential change. Green and blue lines indicate the results of stairway plot and PSMC, respectively, which are obtained from the previous study[22]. Other parameters are the same with Figure 2.

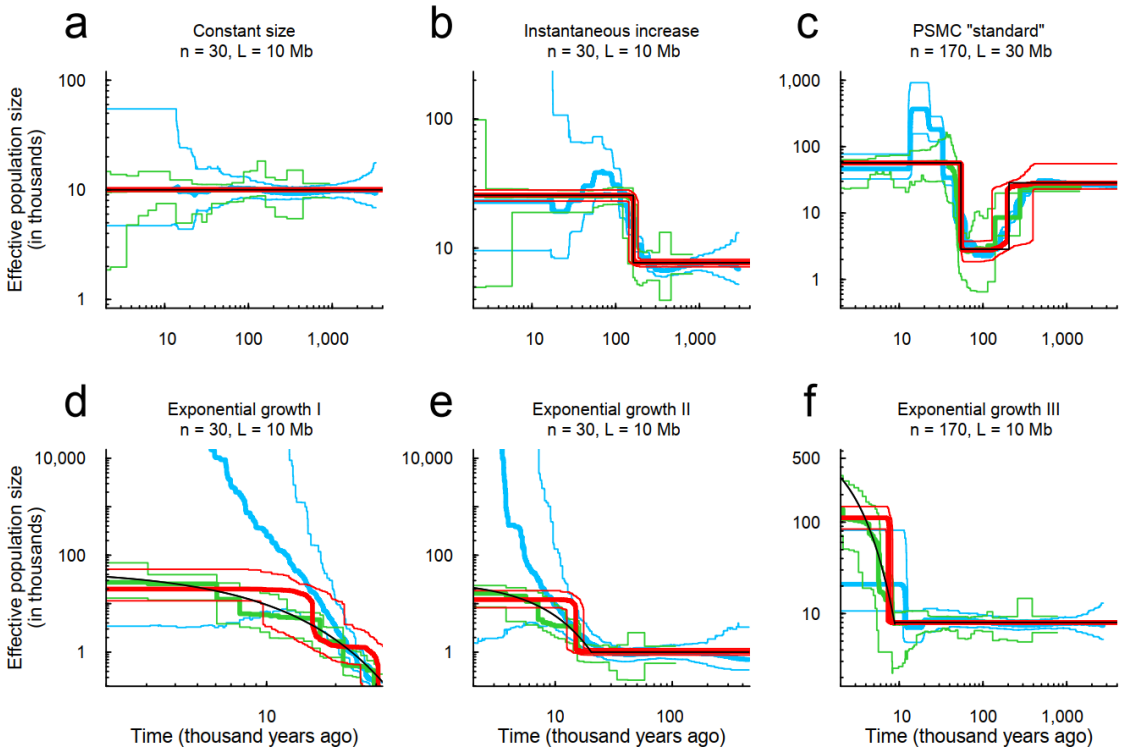

Figure S15. Estimated demographic histories of FitCoal conditional on instantaneous change, stairway plot, and PSMC using simulated samples. (a) Constant size model. (b) Instantaneous increase model. (c) PSMC "standard" model. (d) Exponential growth I model. (e) Exponential growth II model. (f) Exponential growth III model. FitCoal inference was performed conditional on instantaneous change. Other parameters are the same with Figure 2 and S2.

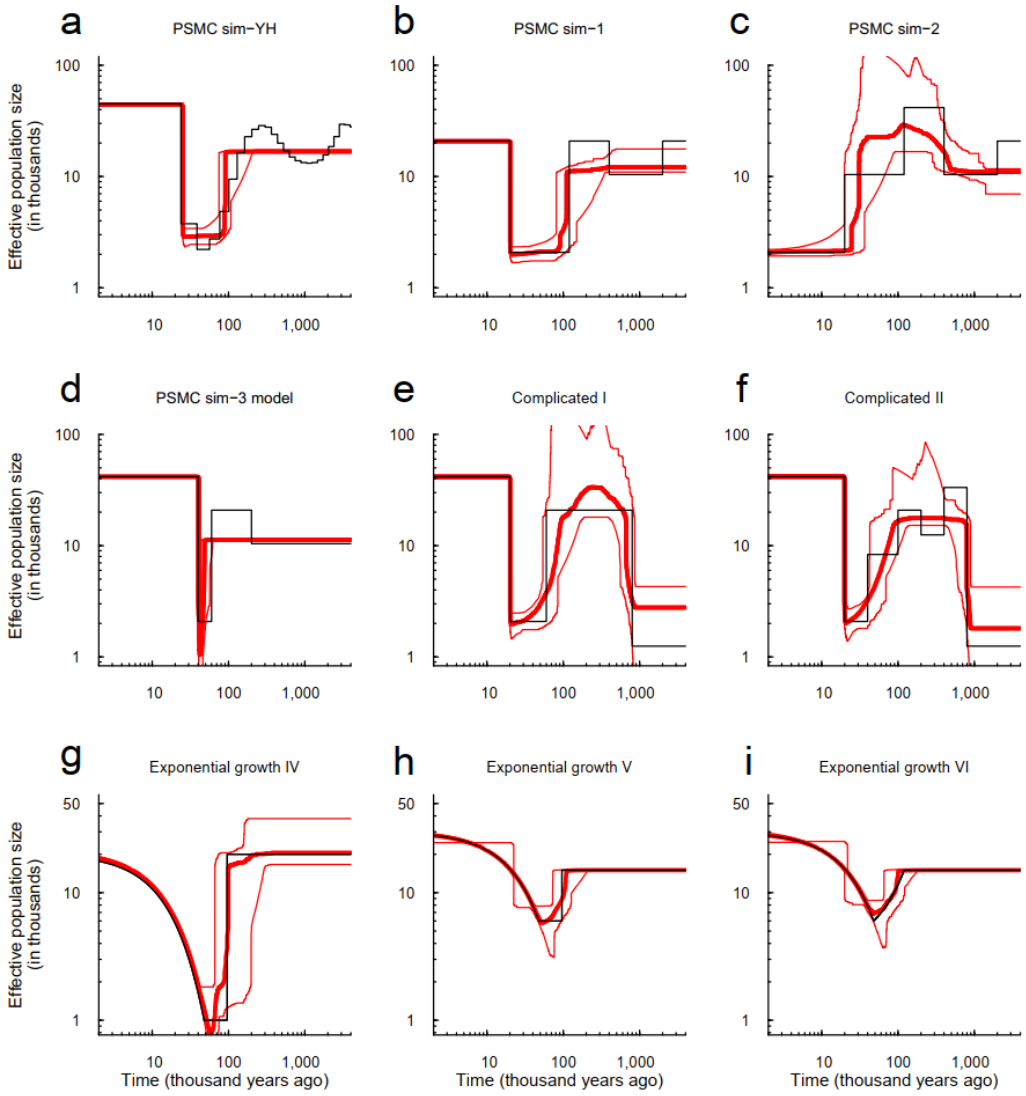

Figure S16. Verification of the accuracy of FitCoal using simulated samples under complex models. (a) PSMC sim-YH model. (b) PSMC sim-1 model. (c) PSMC sim-2 model. (d) PSMC sim-3 model. (e) Complicated I model. (f) Complicated II model. (g) Exponential growth IV model. (h) Exponential growth V model. (i) Exponential growth VI model. Thin black lines indicate true models. Thick red lines are the medians of the estimated histories of FitCoal; thin red lines are 2.5 and 97.5 percentiles of the estimated histories of FitCoal. The number of simulated sequences is 170 and the length of the simulated sequences is 100Mb in all models. Other parameters are the same with Figure 2. The corresponding commands for simulations are described above.

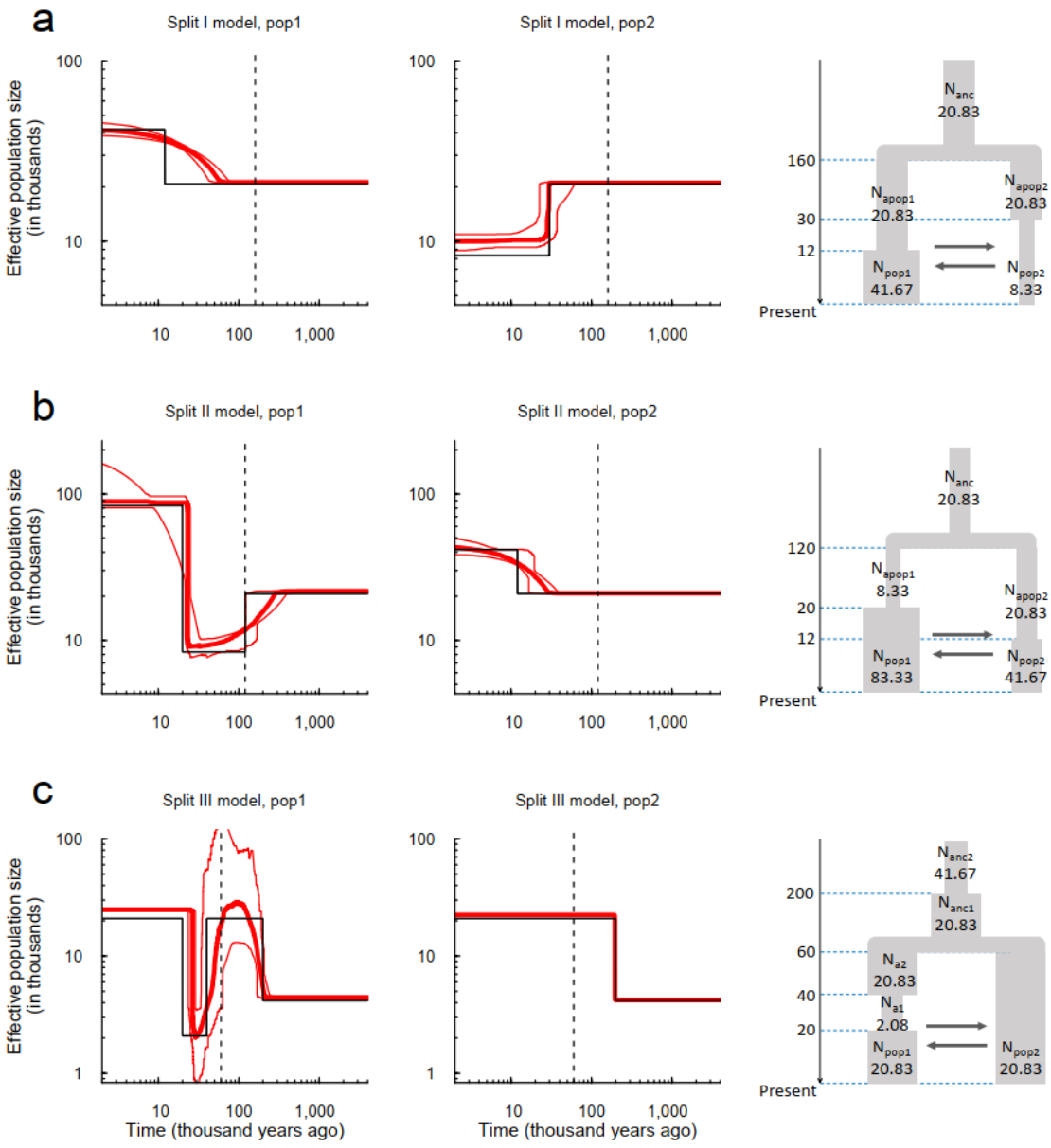

Figure S17. Verification of FitCoal accuracy under three migration models. (a) Inferred histories of two populations under Split I model. The model assumes that the two populations split at 160 kyr ago, and the first population had an instantaneous growth, and the second one had a population size decline. Migration occurred populations. The population size during each stage is shown in the model (the right panel). (b) Inferred histories of two populations under Split II model. (c) Inferred histories of two populations under Split III model. Thin solid black lines indicate true models. Thin dash lines indicate split times. Thick red lines are the medians of the estimated histories of FitCoal; thin red

lines are 2.5 and 97.5 percentiles of the estimated histories of FitCoal. In three rightmost figures, the unit of time is 1,000 years and the unit of population size is 1,000. The number of simulated sequences is 170 and the migration rate ($4Nm$) is 4. The length of the simulated sequences is 30Mb in the first two models and 100MB in the last model. Other parameters are the same with Figure 2. The corresponding commands for simulations are described above.

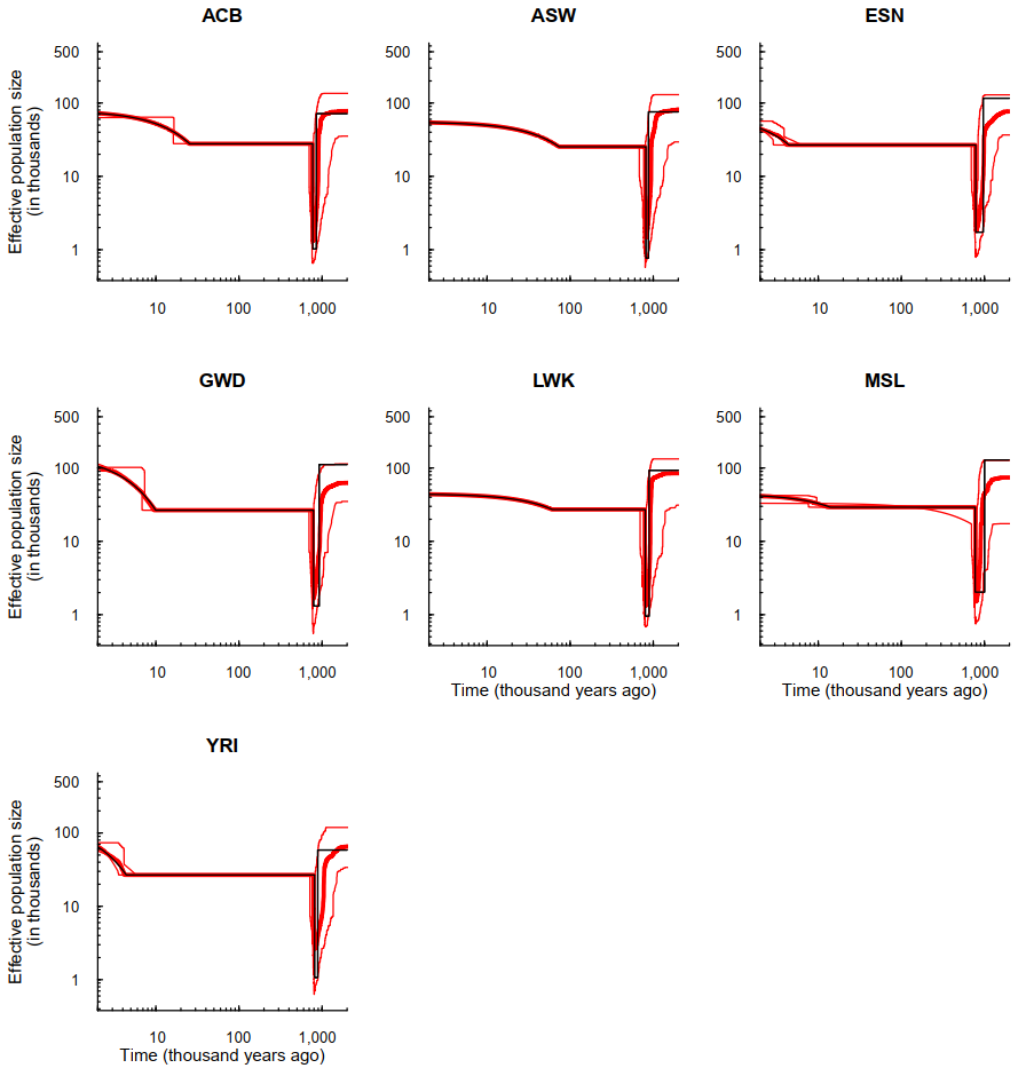

Figure S18. 95% confidence intervals of 1000GP African populations. ACB: African Caribbeans in Barbados; ASW: Americans of African Ancestry in SW USA; ESN: Esan in Nigeria; GWD: Gambian in Western Divisions in the Gambia; LWK: Luhya in Webuye, Kenya; MSL: Mende in Sierra Leone; YRI: Yoruba in Ibadan, Nigeria. The inferred demographic histories in Figure 3 are considered as true models, and 200 simulated samples are obtained for each true model. Black lines indicate true models. Thick red lines are the medians of the estimated histories of FitCoal; thin red lines are 2.5 and 97.5 percentiles of the estimated histories of FitCoal. Truncated SFSs were used. The corresponding commands for simulations are described above.

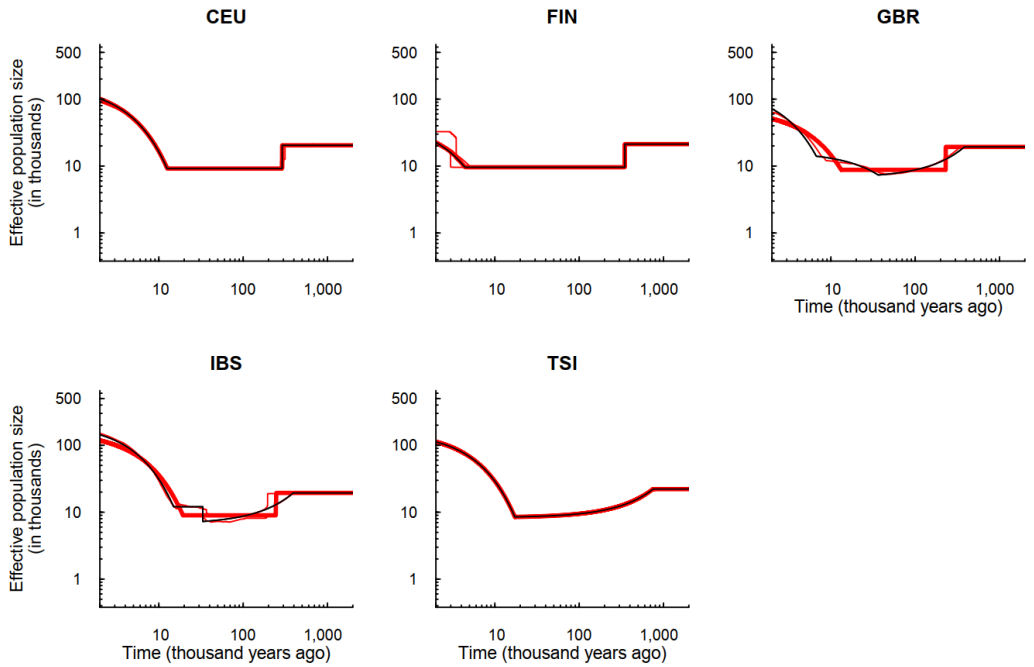

Figure S19. 95% confidence intervals of 1000GP European populations. CEU: Utah Residents (CEPH) with Northern and Western European Ancestry; FIN: Finnish in Finland; GBR: British in England and Scotland; IBS: Iberian Population in Spain; TSI: Toscani in Italia. The inferred demographic histories in Figure 3 are considered as true models, and 200 simulated samples are obtained for each true model. Black lines indicate true models. Thick red lines are the medians of the estimated histories of FitCoal; thin red lines are 2.5 and 97.5 percentiles of the estimated histories of FitCoal. Truncated SFSs were used. The corresponding commands for simulations are described above.

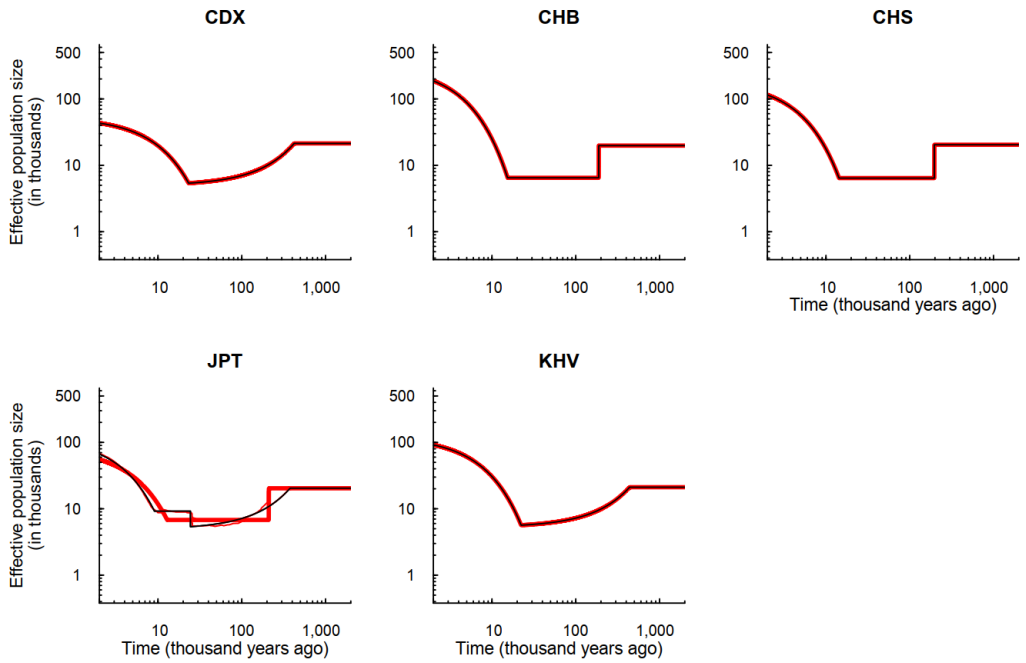

Figure S20. 95% confidence intervals of 1000GP East Asian populations. CDX: Chinese Dai in Xishuangbanna, China; CHB: Han Chinese in Beijing, China; CHS: Southern Han Chinese; JPT: Japanese in Tokyo, Japan; KHV: Kinh in Ho Chi Minh City, Vietnam. The inferred demographic histories in Figure 3 are considered as true models, and 200 simulated samples are obtained for each true model. Black lines indicate true models. Thick red lines are the medians of the estimated histories of FitCoal; thin red lines are 2.5 and 97.5 percentiles of the estimated histories of FitCoal. Truncated SFSs were used. The corresponding commands for simulations are described above.

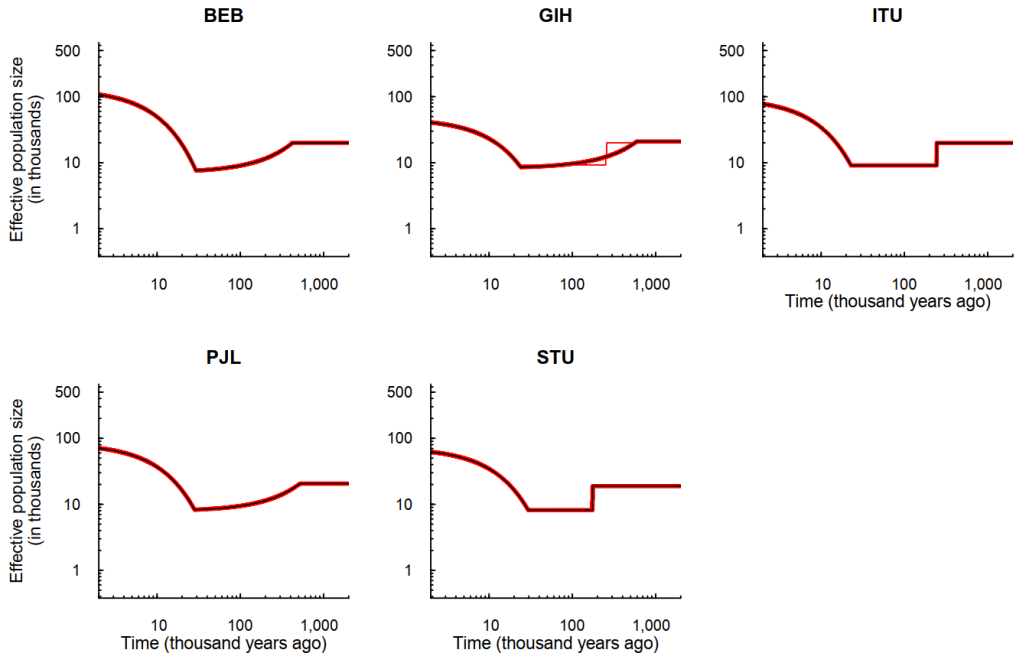

Figure S21. 95% confidence intervals of 1000GP South Asian populations. BEB: Bengali from Bangladesh; GIH: Gujarati Indian from Houston, Texas; ITU: Indian Telugu from the UK; PJL: Punjabi from Lahore, Pakistan; STU: Sri Lankan Tamil from the UK. The inferred demographic histories in Figure 3 are considered as true models, and 200 simulated samples are obtained for each true model. Black lines indicate true models. Thick red lines are the medians of the estimated histories of FitCoal; thin red lines are 2.5 and 97.5 percentiles of the estimated histories of FitCoal. Truncated SFSs were used. The corresponding commands for simulations are described above.

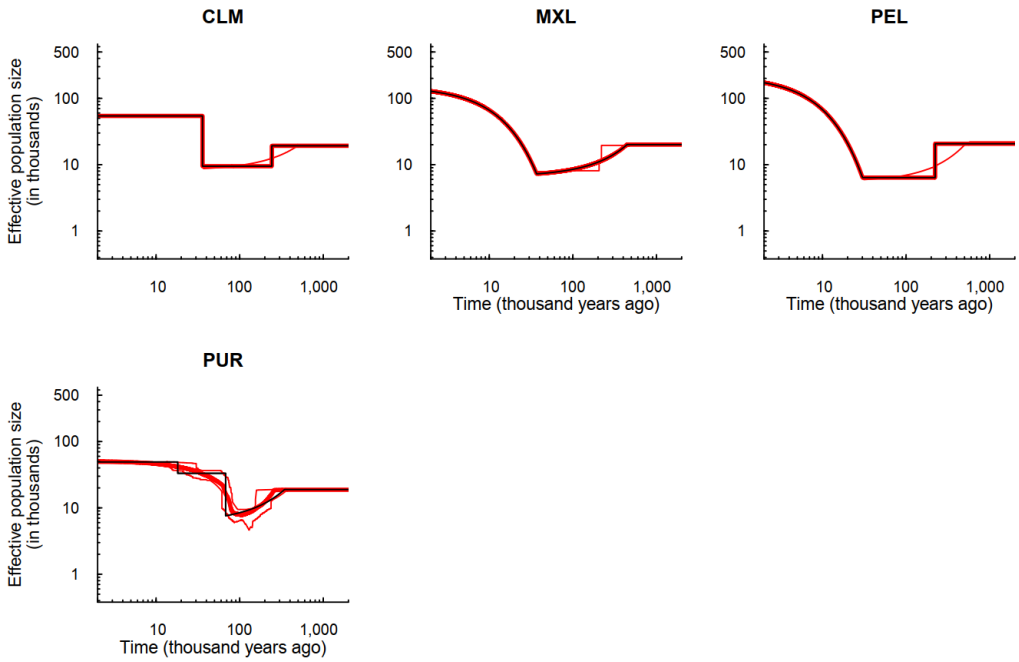

Figure S22. 95% confidence intervals of 1000GP American populations. CLM: Colombians from Medellin, Colombia; MXL: Mexican Ancestry from Los Angeles USA; PEL: Peruvians from Lima, Peru; PUR: Puerto Ricans from Puerto Rico. The inferred demographic histories in Figure 3 are considered as true models, and 200 simulated samples are obtained for each true model. Black lines indicate true models. Thick red lines are the medians of the estimated histories of FitCoal; thin red lines are 2.5 and 97.5 percentiles of the estimated histories of FitCoal. Truncated SFSs were used. The corresponding commands for simulations are described above.

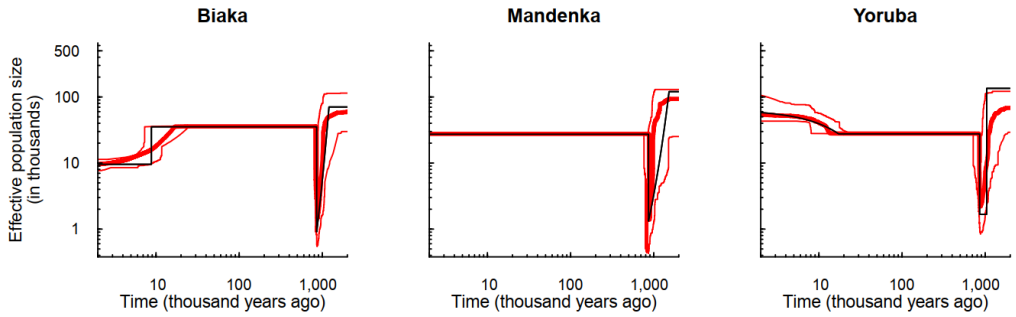

Figure S23. 95% confidence intervals of HGPD-CEPH African populations. The inferred demographic histories in Figure 3 are considered as true models, and 200 simulated samples are obtained for each true model. Black lines indicate true models. Thick red lines are the medians of the estimated histories of FitCoal; thin red lines are 2.5 and 97.5 percentiles of the estimated histories of FitCoal. Truncated SFSs were used. The corresponding commands for simulations are described above.

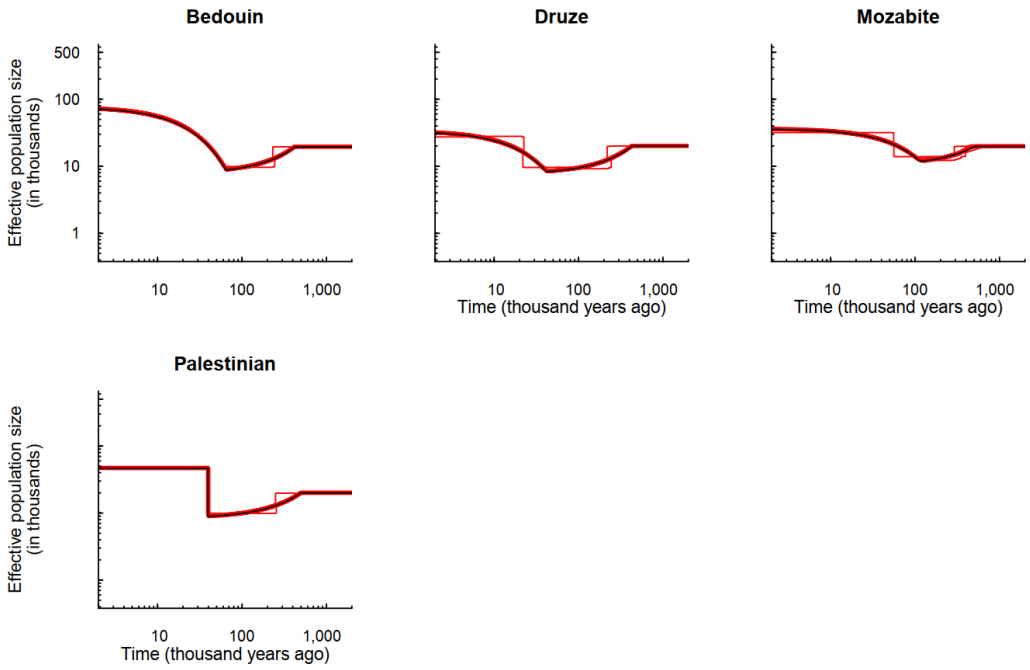

Figure S24. 95% confidence intervals of HGPD-CEPH Middle East populations. The inferred demographic histories in Figure 3 are considered as true models, and 200 simulated samples are obtained for each true model. Black lines indicate true models. Thick red lines are the medians of the estimated histories of FitCoal; thin red lines are 2.5 and 97.5 percentiles of the estimated histories of FitCoal. Truncated SFSs were used. The corresponding commands for simulations are described above.

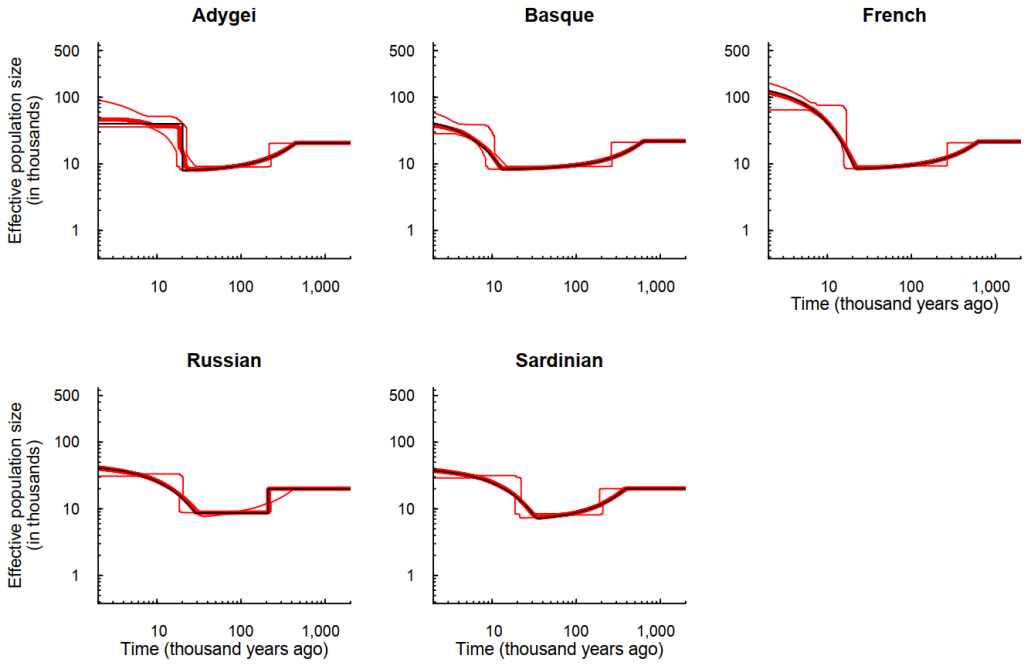

Figure S25. 95% confidence intervals of HGPD-CEPH European populations. The inferred demographic histories in Figure 3 are considered as true models, and 200 simulated samples are obtained for each true model. Black lines indicate true models. Thick red lines are the medians of the estimated histories of FitCoal; thin red lines are 2.5 and 97.5 percentiles of the estimated histories of FitCoal. Truncated SFSs were used. The corresponding commands for simulations are described above.

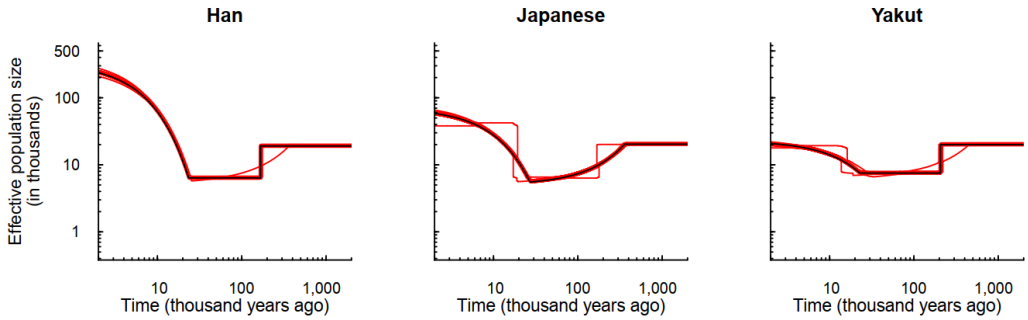

Figure S26. 95% confidence intervals of HGPD-CEPH East Asian populations. The inferred demographic histories in Figure 3 are considered as true models, and 200 simulated samples are obtained for each true model. Black lines indicate true models. Thick red lines are the medians of the estimated histories of FitCoal; thin red lines are 2.5 and 97.5 percentiles of the estimated histories of FitCoal. Truncated SFSs were used. The corresponding commands for simulations are described above.

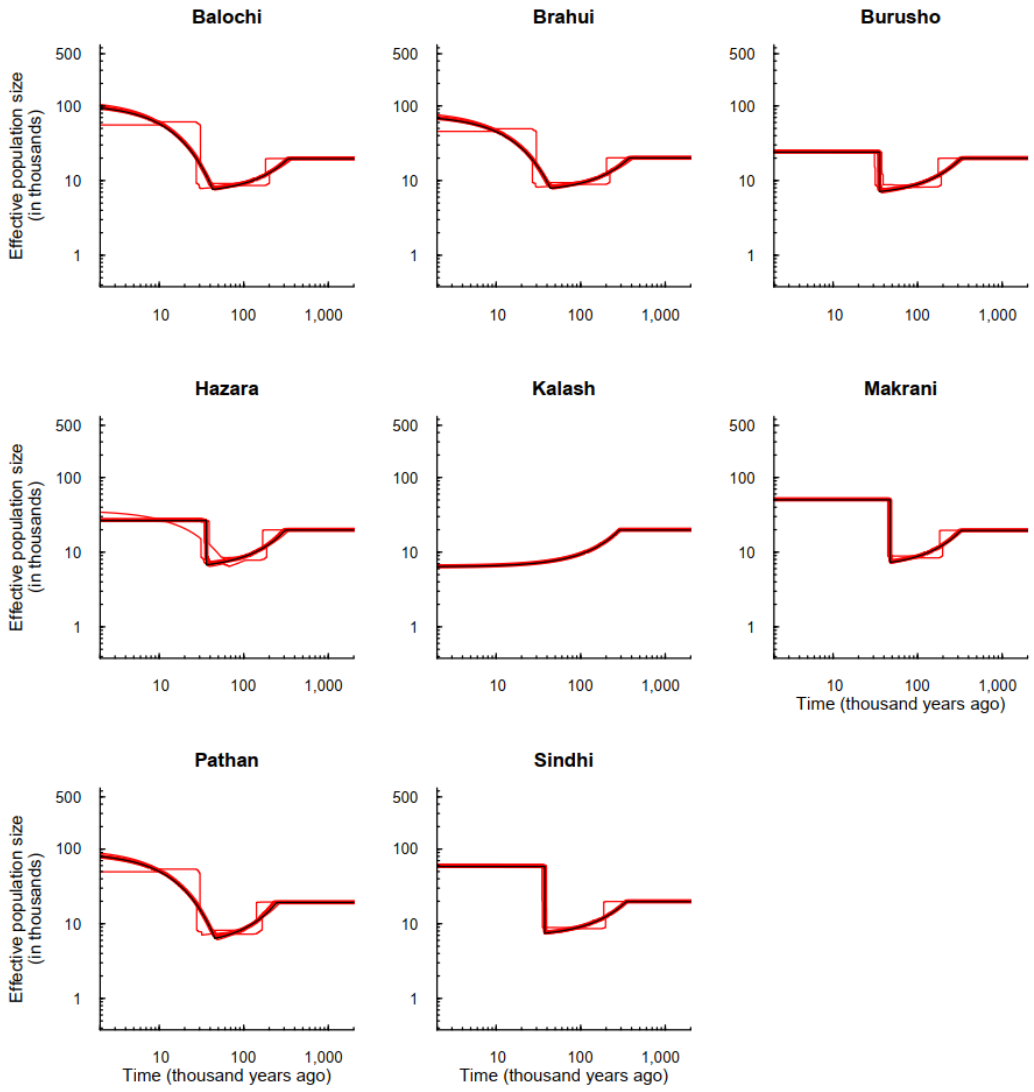

Figure S27. 95% confidence intervals of HGPD-CEPH Central & South Asian populations. The inferred demographic histories in Figure 3 are considered as true models, and 200 simulated samples are obtained for each true model. Black lines indicate true models. Thick red lines are the medians of the estimated histories of FitCoal; thin red lines are 2.5 and 97.5 percentiles of the estimated histories of FitCoal. Truncated SFSs were used. The corresponding commands for simulations are described above.

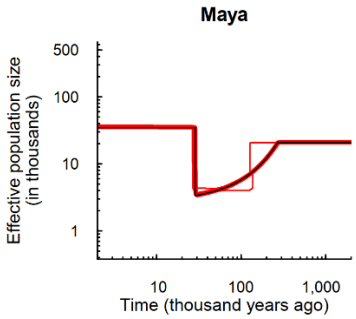

Figure S28. 95% confidence intervals of HGPD-CEPH American population. The inferred demographic history in Figure 3 is considered as the true model, and 200 simulated samples are obtained for the true model. Black line indicates the true model. Thick red line is the median of the estimated histories of FitCoal; thin red lines are 2.5 and 97.5 percentiles of the estimated histories of FitCoal. Truncated SFSs were used. The corresponding command for simulations is described above.

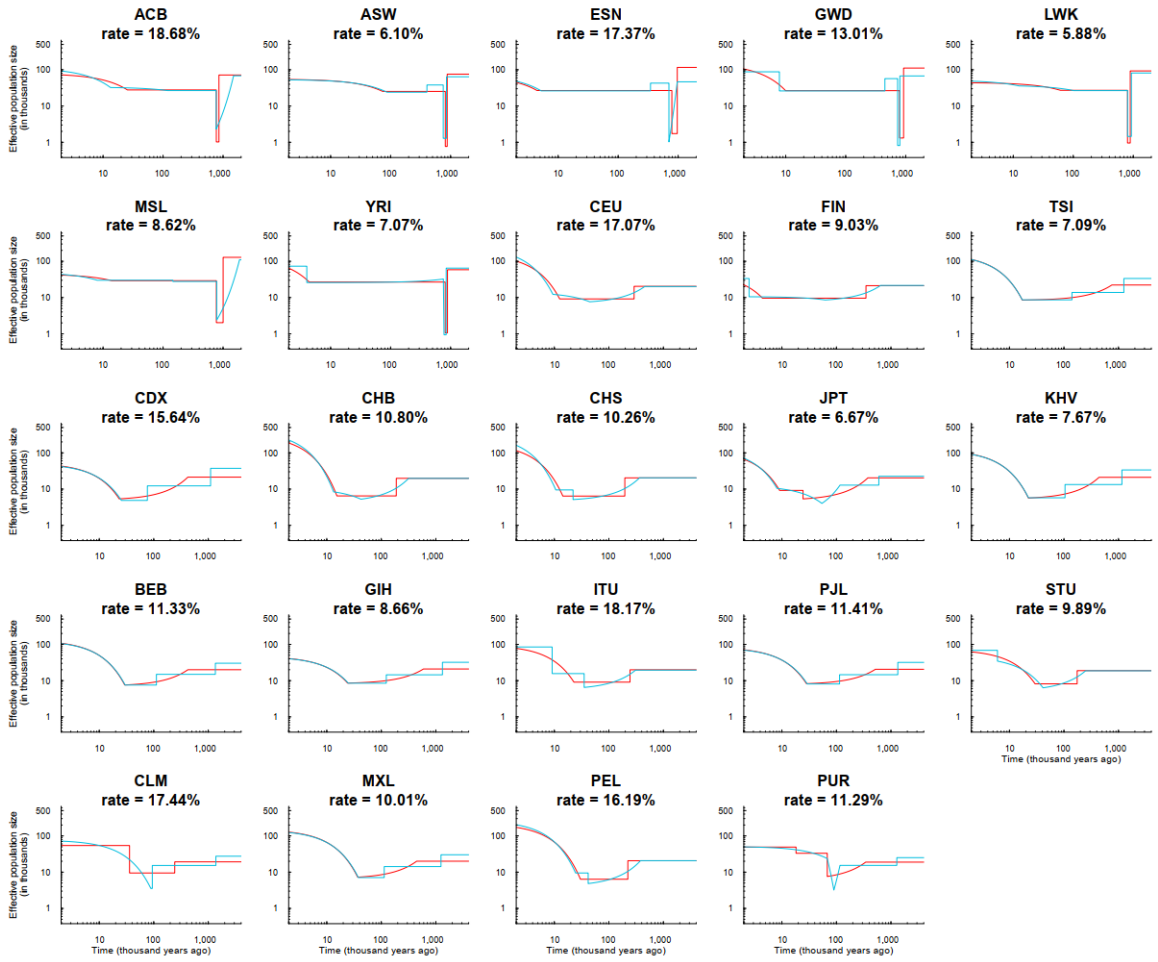

Figure S29. Inferred demographic histories with different inference time intervals of 1000GP populations. Red lines indicate the inferred demographic histories, and blue lines indicate demographic histories with one more inference time interval. The log-likelihood promotion rate for the blue-line-indicating history is presented below the name of population. The results of populations are shown in which log-likelihood promotion rate is at least 5% (Table S16).

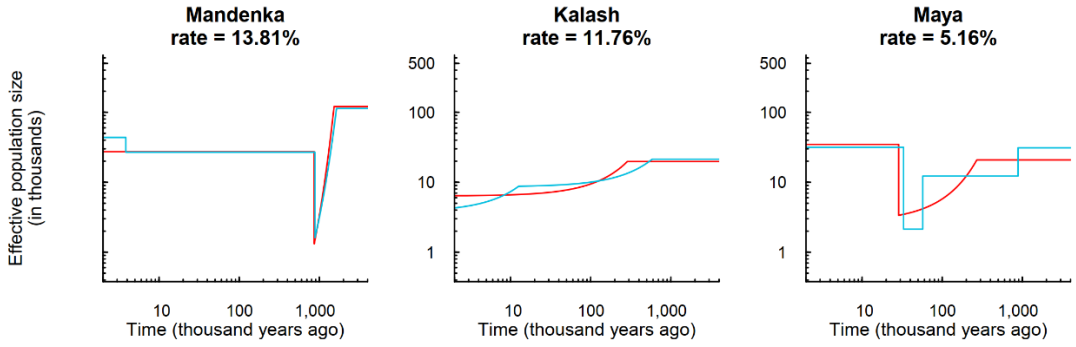

Figure S30. Inferred demographic histories with different inference time intervals of HGPD-CEPH American populations. Red lines indicate the inferred demographic histories, and blue lines indicate demographic histories with one more inference time interval. The log-likelihood promotion rate for the blue-line-indicating history is presented below the name of population. The results of populations are shown in which log-likelihood promotion rate is at least 5% (Table S17).

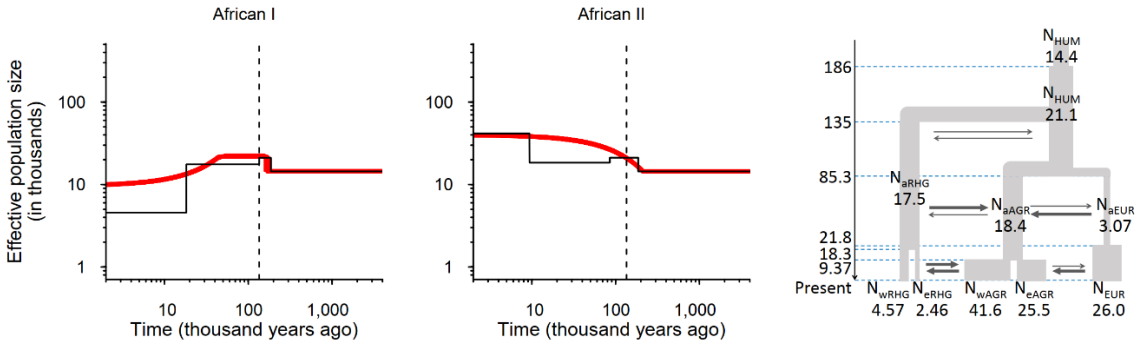

Figure S31. Verification of inference accuracy under complex population structure model. We used FitCoal to estimate the demography of imaginary wRHG (African I population) and wAGR (African II population). Split times and population sizes are show in the right panel. The unit of time is 1,000 years and the unit of population size is 1,000. In the left and middle panel, thin solid black lines indicate true models. Thick red lines are the medians of the estimated histories of FitCoal; thin red lines are 2.5 and 97.5 percentiles of the estimated histories of FitCoal. Truncated SFSs of simulated samples were used to infer the history. The corresponding command for simulations is described above. The number of simulated sequences is 170, and the length of simulated sequences is 800 Mb.

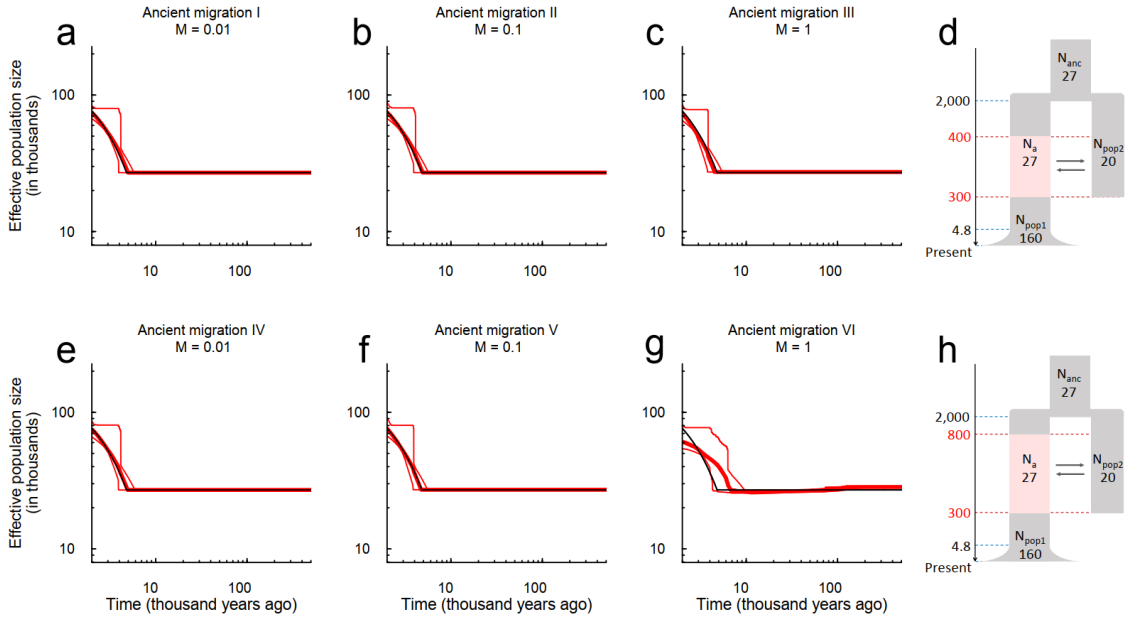

Figure S32. Verification of inference accuracy when migration occurred with unknown hominin population. Two models were considered with different time range of migration between the pop1 and an unknown hominin population (d, h), in which the unit of time is 1,000 years and the unit of population size is 1,000. The region with light red indicates the time range of migration in pop1. We assumed that the unknown population and modern human had common ancestors 2,000 kya. In (d), the unknown population began to migrate with modern human 400 kya, and stopped 300 kya. In (h), the unknown population began to migrate with modern human 800 kya, and stopped 300 kya. M is the migration rate ($4Nm$). The inferred demographic histories of pop1 in (d) are shown in (a – c), and (e – g) are results of pop1 in the second model (h). The number of simulated sequences is 170, and the length of simulated sequences is 800 Mb. Truncated SFSs were used. Thin solid black lines indicate true models. Thick red lines are the medians of the estimated histories of FitCoal; thin red lines are 2.5 and 97.5 percentiles of the estimated histories of FitCoal.

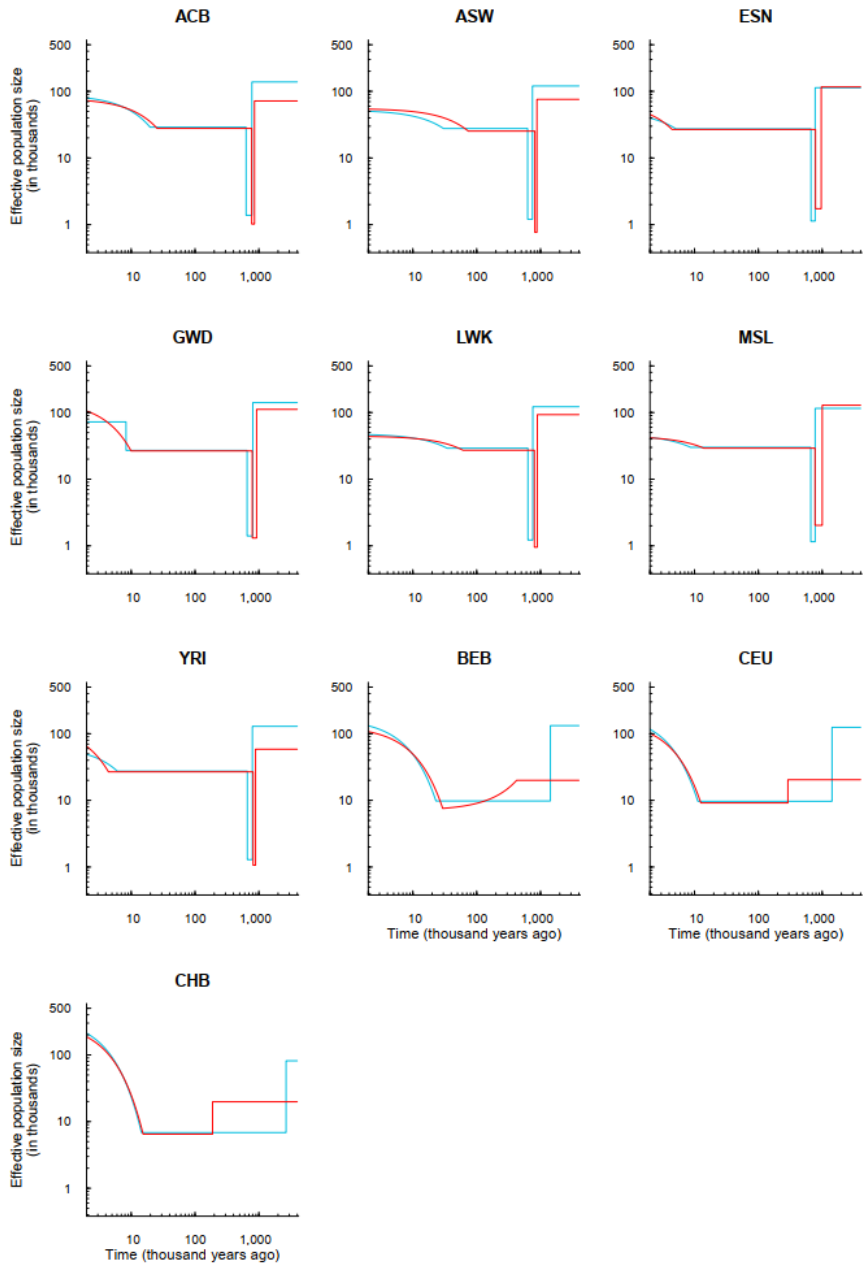

Figure S33. Estimated demographic histories using the full and the truncated SFSs of 1000GP populations. ACB: African Caribbeans in Barbados; ASW: Americans of African Ancestry in SW USA; ESN: Esan in Nigeria; GWD: Gambian in Western Divisions in the Gambia; LWK: Luhya in Webuye, Kenya; MSL: Mende in Sierra Leone; YRI: Yoruba in Ibadan, Nigeria, BEB: Bengali from Bangladesh; CEU: Utah Residents (CEPH) with Northern and Western European Ancestry; CHB: Han Chinese in Beijing, China. The comparison is conducted conditional on the same number of inference time intervals. Red lines indicate the demographic histories inferred using the truncated SFSs,

the same as what were shown in Figure 3a and S9, and blue lines indicate these inferred using the full SFS.

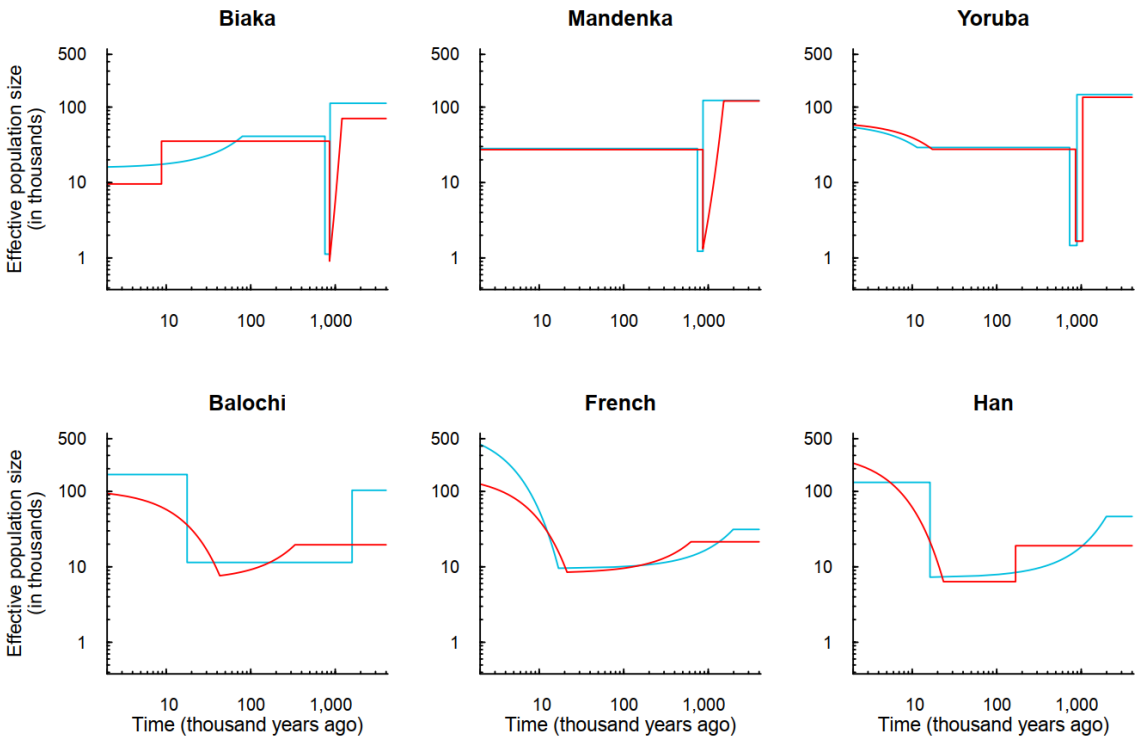

Figure S34. Estimated demographic histories using the full and the truncated SFSs of HGDP-CEPH populations. The comparison is conducted conditional on the same number of inference time intervals. Red lines indicate the demographic histories inferred using the truncated SFSs, the same as what were shown in Figure 3d and S10, and blue lines indicate these inferred using the full SFSs.

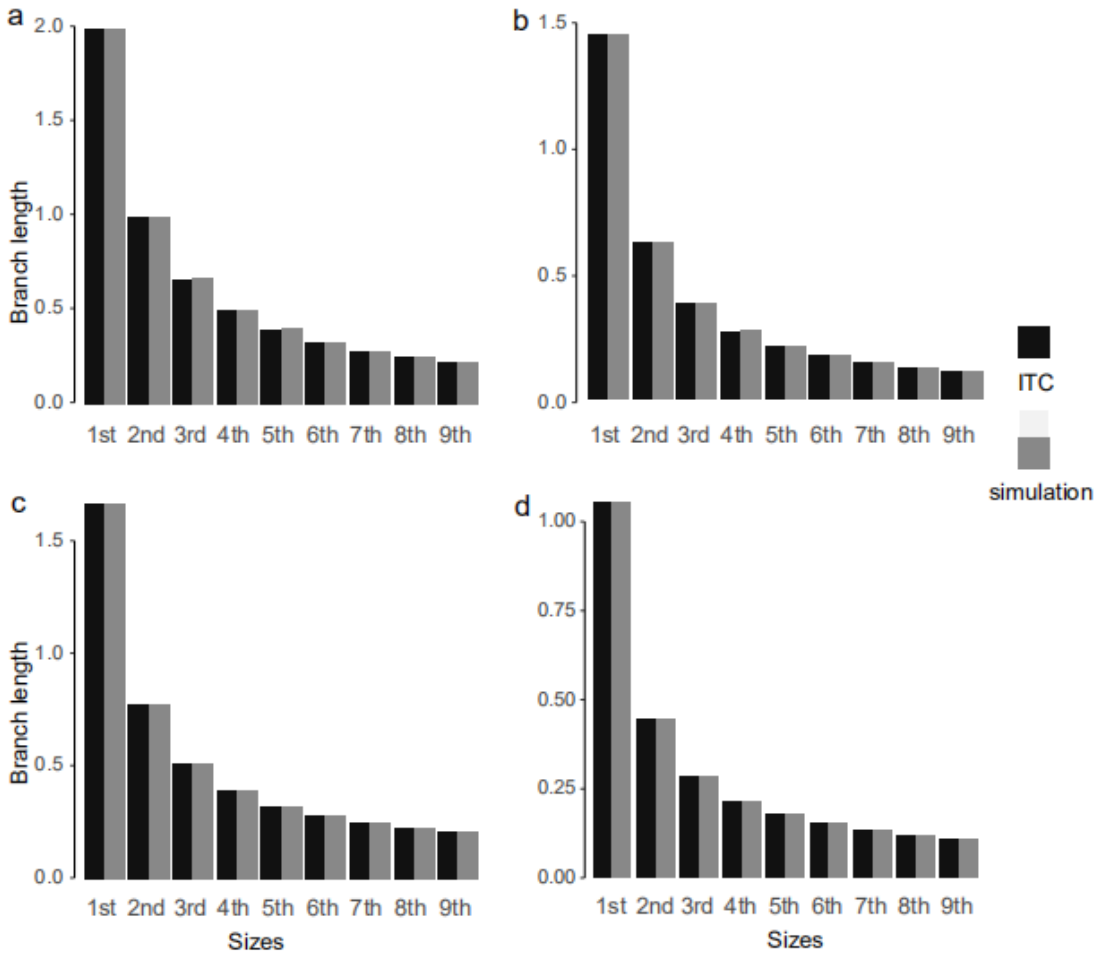

Figure S35. Comparison of the expected branch lengths of FitCoal and the average branch lengths of coalescent simulations. (a) Constant size model. (b) Exponential growth model. (c) Bottleneck model. (d) Complex model. The models, the related parameters, and the ms command lines are described above. $n = 10$. To calculate the average, the number of iterations is 10^6 for coalescent simulations.

Table S1. Proportion of correctly-inferred change type for the most recent demographic event in six models.

Model	Proportion
Constant size	100%
Instantaneous increase	85.5%
PSMC "standard"	100%
Exponential growth I	41.5%
Exponential growth II	61%
Exponential growth III	66.5%

Table S2. Parameters of the super bottleneck in 1000GP African populations.

Population	Ancestral Ne	Start time of the bottleneck		Ne during the bottleneck	End time of the bottleneck		Ne immediate. after the bottleneck
		Time[a]	Change type[b]		Time[a]	Change type[b]	
ACB	71,705	854,288	I	1,021	772,422	I	27,802
ASW	75,746	877,763	I	767	815,473	I	25,302
ESN	116,216	966,439	I	1,735	785,741	I	26,785
GWD	111,486	922,296	I	1,311	790,048	I	26,546
LWK	92,952	891,086	I	954	802,498	I	27,142
MSL	128,666	1,002,553	I	2,031	773,633	I	29,183
YRI	58,563	887,367	I	1,066	812,636	I	26,796

Note: a: Time in years. b: I represents instantaneous change, and E represents exponential change.

Table S3. Parameters of the super bottleneck in HGDP-CEPH African populations.

Population	Ancestral Ne	Start time of the bottleneck		Ne during the bottleneck	End time of the bottleneck		Ne immediately after the bottleneck
		Time[a]	Change type[b]		Time[a]	Change type[b]	
Biaka	70,583	1,202,743	E	908	855,778	I	35,329
Mandenka	120,452	1,526,972	E	1,319	864,078	I	27,306
Yoruba	134,958	1,041,950	I	1,670	856,750	I	27,569

Note: a: Time in years. b: I represents instantaneous change, and E represents exponential change.

Table S4. Parameters of the out-of-Africa bottleneck in 1000GP non-African populations.

Super population	Population	Ancestral Ne	Start time of the bottleneck		Ne during the bottleneck
			Time[a]	Change type[b]	
EUR	CEU	20,414	290,251	I	9,168
	GBR	19,334	383,068	E	7,343
	FIN	21,278	348,509	I	9,612
	IBS	19,393	391,678	E	7,270
	TSI	22,215	756,179	E	8,505
EAS	CDX	20,414	421,701	I	9,168
	CHB	19,334	188,134	E	7,343
	CHS	21,278	196,219	I	9,612
	JPT	19,393	377,347	E	7,270
	KHV	22,215	439,168	E	8,505
SAS	BEB	19,998	422,436	E	7,584
	GIH	20,941	591,769	E	8,554
	ITU	19,912	244,308	I	9,091
	PJL	20,556	518,059	E	8,257
	STU	18,848	174,620	I	8,157
AMR	CLM	19,252	242,526	I	9,482
	MXL	20,063	444,463	E	7,266
	PEL	20,666	222,966	I	6,384
	PUR	18,917	344,023	E	7,606

Note: a: Time in years. b: I represents instantaneous change, and E represents exponential change.

Table S5. Parameters of the out-of-Africa bottleneck in HGDP-CEPH non-African populations.

Super population	Population	Ancestral Ne	Start time of the bottleneck		Ne during the bottleneck
			Time[a]	Change type[b]	
Middle East	Bedouin	19,410	420,348	E	8,793
	Druze	19,930	428,504	E	8,275
	Mozabite	19,932	497,224	E	8,904
	Palestinian	19,733	513,178	E	11,795
European	Adygei	20,467	443,402	E	7,934
	Basque	21,848	627,518	E	8,315
	French	21,469	623,958	E	8,496
	Russian	19,836	209,860	I	8,647
	Sardinian	20,065	385,155	E	7,183
East Asian	Han	19,055	167,289	I	6,365
	Japanese	20,303	357,997	E	5,532
	Yakut	20,012	206,684	I	7,526
Central & South Asian	Balochi	19,618	334,493	E	7,635
	Brahui	20,095	375,825	E	7,897
	Burusho	19,846	325,186	E	7,127
	Hazara	19,765	310,990	E	6,780
	Kalash	19,766	286,505	E	6,346
	Makrani	19,497	324,241	E	7,297
	Pathan	19,283	245,899	E	6,364
	Sindhi	19,758	344,223	E	7,493
American	Maya	20,847	270,478	E	3,365

Note: a: Time in years. b: I represents instantaneous change, and E represents exponential change.

Table S6. The super bottleneck parameters of Bottleneck I model.

Parameter	Value	Median of estimations	Lower bound of 95% CI	Upper bound of 95% CI
Start time of the bottleneck	912,000	978,024	790,776	1,890,528
End time of the bottleneck	792,000	764,376	685,656	794,784
Population size before the bottleneck	93,000	62,224	32,334	130,445
Population size during the bottleneck	1,300	1,907	546	5,838
Population size after the bottleneck	27,000	27,069	26,936	27,230

Table S7. The super bottleneck parameters of Bottleneck IV model.

Parameter	Value	Median of estimations	Lower bound of 95% CI	Upper bound of 95% CI
Start time of the bottleneck	984,000	1,072,368	894,648	1,899,288
End time of the bottleneck	864,000	854,256	774,360	873,672
Population size before the bottleneck	110,000	72,408	31,934	140,463
Population size during the bottleneck	1,300	1,677	638	5,536
Population size after the bottleneck	28,000	27,965	27,817	28,203

Table S8. The super bottleneck parameters of Bottleneck VII model.

Parameter	Value	Median of estimations	Lower bound of 95% CI	Upper bound of 95% CI
Start time of the bottleneck	840,000	887,088	736,560	1,419,480
End time of the bottleneck	720,000	719,712	650,688	1,126,176
Population size before the bottleneck	30,000	31,513	25,356	132,364
Population size during the bottleneck	3,000	2,892	328	7,682
Population size after the bottleneck	30,000	3,0002	29,924	30,086

Table S9. Influence of different log-likelihood promotion thresholds.

Model	30%			20%			10%		
	Underfitting	Correct	Overfitting	Underfitting	Correct	Overfitting	Underfitting	Correct	Overfitting
Constant size	…	100%	0	…	100%	0	…	93%	2%
Instantaneous increase	0	100%	0	0	100%	0	0	99.5%	0.5%
PSMC “standard”	0	100%	0	0	100%	0	0	100%	0
Exponential growth II	0	100%	0	0	100%	0	0	99.5%	0.5%
Exponential growth III	0	100%	0	0	100%	0	0	100%	0
PSMC sim-YH	0	100%	0	0	100%	0	0	99.5%	0.5%
PSMC sim-1	0	100%	0	0	100%	0	0	100%	0
PSMC sim-2	20%	80%	0	0	100%	0	0	100%	0
PSMC sim-3	0	100%	0	0	100%	0	0	98%	2%
Complicated I	0	100%	0	0	100%	0	0	100%	0
Complicated II	0	100%	0	0	100%	0	0	100%	0
Exponential growth IV	0	100%	0	0	100%	0	0	100%	0
Exponential growth V	0	100%	0	0	100%	0	0	100%	0
Exponential growth VI	0	100%	0	0	100%	0	0	100%	0
Split I pop 1	0	100%	0	0	100%	0	0	99.5%	0.5%
Split I pop 2	0	100%	0	0	100%	0	0	99.5%	0.5%
Split II pop 1	0	100%	0	0	100%	0	0	100%	0
Split II pop 2	0	100%	0	0	100%	0	0	100%	0
Split III pop 1	0	100%	0	0	100%	0	0	100%	0
Split III pop 2	0	100%	0	0	100%	0	0	100%	0

Table S10. Information of truncated SFS of 1000GP populations.

Population	Size of SFS $(n-1)$	Truncated sizes of SFS	Proportion of truncated sizes (%)	Proportion of truncated SNPs (%)
ACB	191	171 – 191	10.99	3.17
ASW	121	107 – 121	12.40	3.66
BEB	171	156 – 171	9.36	4.00
CDX	185	174 – 185	6.49	3.56
CEU	197	178 – 197	10.15	4.39
CHB	205	180 – 205	12.68	5.34
CHS	209	191 – 209	9.09	4.17
CLM	187	163 – 187	13.37	5.49
ESN	197	182 – 197	8.12	2.67
FIN	197	181 – 197	8.63	4.19
GBR	181	151 – 181	17.13	6.60
GIH	205	189 – 205	8.29	3.75
GWD	225	208 – 225	8.00	2.59
IBS	213	179 – 213	16.43	6.29
ITU	203	186 – 203	8.87	3.88
JPT	207	182 – 207	12.56	5.26
KHV	197	181 – 197	8.63	4.21
LWK	197	174 – 197	12.18	3.39
MSL	169	147 – 169	13.61	3.63
MXL	127	114 – 127	11.02	5.49
PEL	169	152 – 169	10.65	6.21
PJL	191	177 – 191	7.85	3.54
PUR	207	174 – 207	16.43	5.77
STU	203	171 – 203	16.26	5.79
TSI	213	197 – 213	7.98	3.78
YRI	215	189 – 215	12.56	3.50

Table S11. Proportion of SNPs without or with missing data of HGDP-CEPH populations.

Population	No missing data (%)	Missing samples <= 2 chromosomes (%)
Adygei	92.58	98.80
Balochi	91.01	98.37
Basque	92.66	98.83
Bedouin	87.00	97.30
Biaka	93.25	98.03
Brahui	90.76	98.37
Burusho	91.30	98.55
Druze	89.60	97.86
French	88.78	98.14
Han	84.54	97.14
Hazara	92.53	98.76
Japanese	87.45	97.96
Kalash	90.57	98.48
Makrani	91.10	98.29
Mandenka	91.93	98.13
Maya	94.98	99.13
Mozabite	93.21	98.58
Palestinian	87.22	97.32
Pathan	91.74	98.60
Russian	92.68	98.68
Sardinian	93.04	98.81
Sindhi	90.73	98.43
Yakut	86.66	97.80
Yoruba	92.78	98.02

Table S12. Information of truncated SFS of HGDP-CEPH populations.

Population	Size of SFS $(n-1)$	Truncated sizes of SFS	Proportion of truncated sizes (%)	Proportion of truncated SNPs (%)
Adygei	31	28 – 31	12.90	5.65
Balochi	47	40 – 47	17.02	7.22
Basque	45	41 – 45	11.11	6.18
Bedouin	91	73 – 91	20.88	9.52
Biaka	43	36 – 43	18.60	4.93
Brahui	49	44 – 49	12.24	5.21
Burusho	47	41 – 47	14.89	6.57
Druze	83	70 – 83	16.87	8.24
French	55	50 – 56	10.91	5.59
Han	85	67 – 85	22.35	8.72
Hazara	37	32 – 37	16.22	6.72
Japanese	53	45 – 53	16.98	6.95
Kalash	43	40 – 43	9.30	5.22
Makrani	49	41 – 49	18.37	7.24
Mandenka	43	37 – 43	16.28	4.75
Maya	41	37 – 41	12.20	7.20
Mozabite	53	44 – 53	18.87	7.43
Palestinian	91	78 – 91	15.38	8.53
Pathan	47	35 – 49	27.66	10.12
Russian	49	40 – 49	20.41	8.06
Sardinian	55	51 – 55	27.27	11.65
Sindhi	47	41 – 47	14.89	6.35
Yakut	49	39 – 49	22.45	10.02
Yoruba	43	38 – 43	13.95	4.14

Table S13. Comparison of branch length between theoretical values and FitCoal under the constant size model.

$n = 5$		
Type	Theoretical length	FitCoal length
1	2.000000000000	1.999999995001
2	1.000000000000	0.999999995001
3	0.666666666667	0.666666661667
4	0.500000000000	0. 499999995000
$n = 1{,}000$		
Type	Theoretical length	FitCoal length
1	2.000000000000	1.999999999979
100	0.020000000000	0.019999999980
200	0.010000000000	0.009999999980
300	0.006666666667	0.006666666647
400	0.005000000000	0.004999999980
500	0.004000000000	0.003999999980
600	0.003333333333	0.003333333313
700	0.002857142857	0.002857142837
800	0.002500000000	0.002499999980
900	0.002222222222	0.002222222202
999	0.002002002002	0.002002001982

Table S14. Comparison of accuracy between FitCoal and Z-W's method.

Constant size model			
size	Z-W's method	FitCoal	Tabulated FitCoal
1	1.9999999999	1.9999999977	2.0000000000
2	0.9999999999	0.9999999977	1.0000000000
3	0.6666666666	0.6666666644	0.6666666666
4	0.4999999999	0.4999999977	0.5000000000
5	0.3999999999	0.3999999977	0.4000000000
6	0.3333333333	0.3333333311	0.3333333333
7	0.2857142857	0.2857142834	0.2857142857
8	0.2499999999	0.2499999977	0.2500000000
9	0.2222222222	0.2222222200	0.2222222222
Instantaneous growth model			
size	Z-W's method	FitCoal	Tabulated FitCoal
1	1.7547171613	1.7547178684	1.7547229380
2	0.7797340922	0.7797345132	0.7797375358
3	0.4686921135	0.4686923318	0.4686939043
4	0.3218480766	0.3218481580	0.3218487511
5	0.2394397929	0.2394397884	0.2394397658
6	0.1883537444	0.1883536920	0.1883533260
7	0.1545070379	0.1545069652	0.1545064537
8	0.1309436073	0.1309435332	0.1309430117
9	0.1138668845	0.1138668210	0.1138663751
Bottleneck model			
size	Z-'s method	FitCoal	FitCoal with tabulated
1	1.6737287481	1.6737298163	1.6737374623
2	0.7744529188	0.7744529447	0.7744538197
3	0.5109730563	0.5109727763	0.5109715354
4	0.3927621211	0.3927618350	0.3927603900
5	0.3264269184	0.3264267194	0.3264256821
6	0.2832102142	0.2832101093	0.2832095492
7	0.2519772704	0.2519772388	0.2519770488
8	0.2277455013	0.2277455192	0.2277455704
9	0.2080244642	0.2080245126	0.2080247051

Table S15. Comparison of accuracy between FitCoal and simulations.

Constant size model			
Type	Simulation method	FitCoal	Tabulated FitCoal
1	1.999529551	1.999999998	2.000000000
2	0.999720720	0.999999998	1.000000000
3	0.667102715	0.666666664	0.666666667
4	0.500240165	0.499999998	0.500000000
5	0.400967708	0.399999998	0.400000000
6	0.333256388	0.333333331	0.333333333
7	0.285465389	0.285714283	0.285714286
8	0.249471384	0.249999998	0.250000000
9	0.222272679	0.222222220	0.222222222
Exponential growth model			
Type	Simulation method	FitCoal	Tabulated FitCoal
1	1.441789518	1.441679286	1.441673129
2	0.616556332	0.616509230	0.616508244
3	0.376438453	0.376743719	0.376742859
4	0.269168704	0.268510898	0.268510338
5	0.207984340	0.208373433	0.208373096
6	0.170848693	0.170519845	0.170519652
7	0.144555420	0.144603196	0.144603091
8	0.125837330	0.125751961	0.125751908
9	0.111364011	0.111402468	0.111402445
Bottleneck model			
Type	Simulation method	FitCoal	Tabulated FitCoal
1	1.673321651	1.673732814	1.673741394
2	0.775051787	0.774454488	0.774457584
3	0.510960086	0.510973534	0.510974557
4	0.394262151	0.392762187	0.392762519
5	0.325116671	0.326426872	0.326426966
6	0.284039310	0.283210170	0.283210115
7	0.251717509	0.251977260	0.251977042
8	0.228240338	0.227745526	0.227745129
9	0.207539986	0.208024514	0.208023953
Complex model			

Type	Simulation method	FitCoal	Tabulated FitCoal
1	1.055607245	1.055618949	1.055592252
2	0.444340081	0.444811898	0.444812747
3	0.285522751	0.285500848	0.285501081
4	0.215995323	0.215622334	0.215622470
5	0.176447487	0.176540313	0.176540331
6	0.151750997	0.151231386	0.151231289
7	0.133173783	0.133109963	0.133109779
8	0.118845125	0.119172606	0.119172375
9	0.107810932	0.107899199	0.107898957

1272

Table S16. Likelihood promotion rate of inferred demographic histories with different inference time intervals of 1000GP populations.

Super population	Population	Rate compared with result of (*k*-1) inference time intervals (%)			
		2	3	4	5
AFR	ACB	1384.26	350.31	60.09	18.68
	ASW	3538.08	130.56	93.48	6.10
	ESN	714.05	35.23	126.18	17.37
	GWD	590.15	302.50	112.43	13.01
	LWK	2925.80	91.55	70.91	5.88
	MSL	2935.78	43.91	60.37	8.62
	YRI	861.84	166.36	69.09	7.07
EUR	CEU	135.51	2471.16	17.07	…
	FIN	341.55	541.28	9.03	…
	GBR	65.68	2900.65	22.20	2.50
	IBS	384.43	2289.75	25.85	4.34
	TSI	236.98	2286.49	7.09	…
EAS	CDX	49.99	4430.87	15.64	…
	CHB	175.03	5343.87	10.80	…
	CHS	111.49	4384.47	10.26	…
	JPT	56.37	4100.17	24.05	6.76
	KHV	153.13	4242.29	7.67	…
SAS	BEB	319.95	2491.42	11.33	…
	GIH	101.31	1982.75	8.66	…
	ITU	261.16	1836.98	18.17	…
	PJL	254.33	1884.50	11.41	…
	STU	284.42	2590.84	9.89	…
AMR	CLM	834.67	1867.06	17.44	…
	MXL	347.01	4258.47	10.01	…
	PEL	359.65	5549.64	16.19	…
	PUR	1335.08	967.44	22.39	11.29

Table S17. Likelihood promotion rate of inferred demographic histories with different inference time intervals of HGDP-CEPH populations.

Super population	Population	Rate compared with result of (*k*-1) inference time intervals (%)			
		2	3	4	5
AFR	Biaka	387.67	931.28	58.4	0.42
	Mandenka	2350.47	31.56	13.81	…
	Yoruba	3157.91	24.28	67.73	0.35
ME	Bedouin	282.02	87.97	1.89	…
	Druze	33.15	218.35	1.68	…
	Mozabite	275.41	130.64	2.99	…
	Palestinian	195.99	102.86	1.2	…
EUR	Adygei	179.37	98.23	0.37	…
	Basque	336.87	42.2	0.78	…
	French	48.25	201.88	0.58	…
	Russian	75.68	97.53	0.27	…
	Sardinian	105.69	649.27	1.04	…
EAS	Han	59.53	201.39	0.95	…
	Japanese	86.6	154.89	0.41	…
	Yakut	287.46	43.19	0.23	…
CSA	Balochi	40.25	244.48	0.78	…
	Brahui	27.24	276.49	0.6	…
	Burusho	75.72	115.73	0.21	…
	Hazara	95.97	159.24	1.05	…
	Kalash	1465.6	11.76	…	…
	Makrani	106.68	112.25	0.35	…
	Pathan	28.68	218.83	0.31	…
	Sindhi	69.31	170.14	0.29	…
AMR	Maya	136.19	1813.04	5.16	…

Table S18. Probabilities of each state (the number of ancestral lineages remained) at time *t*.

Standard coalescent time	*n*	Number of ancestral lineages remained							
		1	2	3	4	5	6	7	else
0.6	30	1.92%	17.22%	38.16%	30.57%	10.39%	1.62%	0.12%	<0.01%
0.6	40	1.64%	15.62%	36.9%	31.85%	11.78%	2.03%	0.17%	0.01%
0.6	50	1.49%	14.67%	36.06%	32.55%	12.68%	2.32%	0.21%	0.01%
0.6	180	1.11%	12.05%	33.27%	34.28%	15.53%	3.37%	0.37%	0.02%
0.6	200	1.09%	11.96%	33.15%	34.34%	15.65%	3.42%	0.38%	0.02%
0.6	220	1.08%	11.88%	33.05%	34.38%	15.74%	3.46%	0.38%	0.02%
0.8	30	7.32%	36.36%	40.14%	14.22%	1.86%	0.1%	<0.01%	<0.01%
0.8	40	6.73%	34.93%	40.68%	15.36%	2.17%	0.12%	<0.01%	<0.01%
0.8	50	6.38%	34.05%	40.96%	16.08%	2.38%	0.14%	<0.01%	<0.01%
0.8	180	5.44%	31.41%	41.56%	18.27%	3.09%	0.22%	0.01%	<0.01%
0.8	200	5.4%	31.31%	41.58%	18.36%	3.12%	0.22%	0.01%	<0.01%
0.8	220	5.37%	31.22%	41.59%	18.43%	3.15%	0.22%	0.01%	<0.01%
1.0	30	15.99%	48.88%	29.75%	5.09%	0.28%	0.01%	<0.01%	<0.01%
1.0	40	15.18%	48.17%	30.73%	5.58%	0.33%	0.01%	<0.01%	<0.01%
1.0	50	14.7%	47.72%	31.32%	5.89%	0.36%	0.01%	<0.01%	<0.01%
1.0	180	13.35%	46.29%	33%	6.88%	0.48%	0.01%	<0.01%	<0.01%
1.0	200	13.29%	46.23%	33.06%	6.92%	0.48%	0.01%	<0.01%	<0.01%
1.0	220	13.25%	46.18%	33.12%	6.95%	0.49%	0.01%	<0.01%	<0.01%
1.2	30	26.31%	53.05%	18.95%	1.65%	0.04%	<0.01%	<0.01%	<0.01%
1.2	40	25.42%	52.97%	19.75%	1.82%	0.05%	<0.01%	<0.01%	<0.01%
1.2	50	24.89%	52.89%	20.23%	1.93%	0.05%	<0.01%	<0.01%	<0.01%
1.2	180	23.37%	52.6%	21.69%	2.27%	0.07%	<0.01%	<0.01%	<0.01%
1.2	200	23.31%	52.59%	21.74%	2.29%	0.07%	<0.01%	<0.01%	<0.01%
1.2	220	23.26%	52.58%	21.79%	2.3%	0.07%	<0.01%	<0.01%	<0.01%

Note: the highlighted area represents that, when $t \geq 1.0$, the number of ancestral lineages remained is no more than 3 in more than 90% cases.

References

1 Fu, Y. X. Statistical properties of segregating sites. *Theor. Popul. Biol.* **48**, 172-197 (1995).

2 Zivković, D. & Wiehe, T. Second-order moments of segregating sites under variable population size. *Genetics* **180**, 341-357 (2008).

3 Li, H. & Stephan, W. Inferring the demographic history and rate of adaptive substitution in *Drosophila*. *PLoS Genet.* **2**, e166 (2006).

4 Hudson, R. R. Two-locus sampling distributions and their application. *Genetics* **159**, 1805-1817 (2001).

5 Kim, Y. & Stephan, W. Detecting a local signature of genetic hitchhiking along a recombining chromosome. *Genetics* **160**, 765-777 (2002).

6 Fay, J. C. & Wu, C.-I. Hitchhiking under positive Darwinian selection. *Genetics* **155**, 1405-1413 (2000).

7 Fu, Y. X. & Li, W. H. Statistical tests of neutrality of mutations. *Genetics* **133**, 693-709 (1993).

8 Tajima, F. Statistical method for testing the neutral mutation hypothesis by DNA polymorphism. *Genetics* **123**, 585-595 (1989).

9 Polanski, A., Bobrowski, A. & Kimmel, M. A note on distributions of times to coalescence, under time-dependent population size. *Theor. Popul. Biol.* **63**, 33-40 (2003).

10 Bhaskar, A. & Song, Y. S. Descartes' rule of signs and the identifiability of population demographic models from genomic variation data. *Ann. Stat.* **42**, 2469-2493 (2014).

11 Hsieh, P. *et al.* Model-based analyses of whole-genome data reveal a complex evolutionary history involving archaic introgression in Central African Pygmies. *Genome Res.* **26**, 291-300 (2016).

12 Lopez, M. *et al.* The demographic history and mutational load of African hunter-gatherers and farmers. *Nat. Ecol. Evol.* **2**, 721-730 (2018).

13 Schlebusch, C. M. & Jakobsson, M. Tales of human migration, admixture, and selection in Africa. *Annu. Rev. Genomics Hum. Genet.* **19**, 405-428 (2018).

14 Skoglund, P. *et al.* Reconstructing prehistoric African population structure. *Cell* **171**, 59-71 (2017).

15 Durvasula, A. & Sankararaman, S. Recovering signals of ghost archaic introgression in African populations. *Sci. Adv.* **6**, eaax5097 (2020).

16 Beerli, P. Effect of unsampled populations on the estimation of population sizes and migration rates between sampled populations. *Mol. Ecol.* **13**, 827-836 (2004).

17 Hudson, R. R. Generating samples under a Wright-Fisher neutral model of genetic variation. *Bioinformatics* **18**, 337-338 (2002).

18 Chen, G. K., Marjoram, P. & Wall, J. D. Fast and flexible simulation of DNA sequence data. *Genome Res.* **19**, 136-142 (2009).

19 Boyko, A. R. *et al.* Assessing the evolutionary impact of amino acid mutations in the human genome. *PLoS Genet.* **4**, e1000083 (2008).
20 Li, H. & Durbin, R. Inference of human population history from individual whole-genome sequences. *Nature* **475**, 493-496 (2011).
21 Gutenkunst, R. N., Hernandez, R. D., Williamson, S. H. & Bustamante, C. D. Inferring the joint demographic history of multiple populations from multidimensional SNP frequency data. *PLoS Genet.* **5**, e1000695 (2009).
22 Liu, X. M. & Fu, Y. X. Exploring population size changes using SNP frequency spectra. *Nat. Genet.* **47**, 555-559 (2015).